Supporting Information

A chemo-selective deprotection–cyclization strategy enables fluorescent imaging of hydroxylamine and reveals its pathologic role in Parkinson's disease

Shunping Zang,[a†] Jia Ke,[b†] Hanbing Zheng,[a] Qing Liu,[a] Liu Yang,[a] Chaoyi Yao,[a*] Benhua Wang,[a*] Minhuan Lan,[a] and Xiangzhi Song[a*]

[a] College of Chemistry and Chemical Engineering, Central South University, Changsha, Hunan 410083, P.R. China
[b] Liangzhu Laboratory, Zhejiang University Medical Center, Hangzhou, Zhejiang 311121, P.R. China

[†] These authors contributed equally to this work.

*Corresponding authors: chaoyiyao@csu.edu.cn; benhuawang@csu.edu.cn; xzsong@csu.edu.cn

1. Experimental Sections

1.1 Materials and reagents

All commercial solvents and chemicals were used without further purification. TLC plates and silica gel (100~200 mesh) were purchased from Qingdao Ocean Chemicals (Qingdao, China).

1.2 Instruments

^{1}H NMR and ^{13}C NMR spectra were obtained using a Bruker 400 spectrometer. Mass spectra were obtained using a Bruker Daltonics micro-TOF-Q II spectrometer. Fluorescence spectra were recorded on a Hitachi F-7000 fluorometer, and UV-*vis* absorption spectra were recorded on a Shimadzu UV-2450 spectrophotometer. Cell imaging experiments were performed on an Olympus FV3000 confocal microscope. Tissue slice imaging was carried out using an Olympus VS200 digital slice scanner. Living mice imaging was conducted with AniView100 living imaging system. Western blot assays were performed using ChemiDoc Touch Imaging System (Bio-Rad, USA).

1.3 Spectroscopic methods

Each fluorescent probe was dissolved in DMSO to prepare a 1.0 mM stock solution. For the spectral tests, the concentration of each sensor was adjusted to 10.0 μM in PBS buffer (pH = 7.4, 10 mM). The solutions of HA and other analytes at defined concentrations were prepared and added in an appropriate amount to the sensor solution. All absorption and fluorescence spectra were recorded at room temperature. The excitation wavelengths varied depending on each probe: **Cou-HA**, λ_{ex} = 405 nm; **Fluo-HA**, λ_{ex} = 450 nm; **Naph-HA**, λ_{ex} = 420 nm and **DCI-HA-n**, λ_{ex} = 480 nm.

1.4 Determination of detection limit (LOD)

LOD was determined from the fluorescence titration data. LOD was calculated according to the following equation (1):

$$\mathrm{LOD} = \frac{3\sigma}{k} \quad (1)$$

where σ is the standard deviation of the blank sample (n = 15), and k is the slope between the fluorescence intensity versus concentration.

1.5 Cytotoxicity assay

The biocompatibility of probe **DCI-HA-2** was evaluated using MTT assay. PC-12 cells were seeded on a 96-well plate at a density of 8×10^3 cells/well in 200.0 μL of culture medium and allowed to attach overnight. Then, the cells were exposed to various concentrations of **DCI-HA-2** (0, 5.0, 10.0, 15.0, 20.0, 25.0 μM) for 24 h. After that, 20.0 μL of MTT solution (5.0 mg/mL in PBS) was added to each well, and the plate was incubated at 37 °C in a 5% CO_2 atmosphere for another 4 h. Subsequently, the solution in each well was carefully aspirated, and 200.0 μL of DMSO was added to dissolve the formazan crystals. The absorbance at 570 nm was measured. The relative cell viability (%) was calculated by the following formula (2):

$$\text{Cell viability (\%)} = \frac{\mathrm{OD_{sample}}}{\mathrm{OD_{control}}} \times 100\% \quad (2)$$

where $\mathrm{OD_{sample}}$ and $\mathrm{OD_{control}}$ represent the optical density values of the treatment group and the control group, respectively.

1.6 Imaging of exogenous and endogenous HA in PC-12 cells

PC-12 cell lines were cultured in DMEM containing 10% FBS, 100.0 U/mL penicillin, and 100.0 μg/mL streptomycin. Cells were placed in an incubator at 37 °C with 5% CO_2 and 99% humidity.

For exogenous HA imaging, PC-12 cells were pre-treated with various concentrations of HA (0, 5.0, 10.0, 20.0 and 40.0 μM) for 1 h and then stained with **DCI-HA-2** (10.0 μM) for 30 min.

For endogenous HA imaging, PC-12 cells were directly treated with L-arginine (L-Arg) (50.0 and 100.0 μM) for 4 h and subsequently stained with **DCI-HA-2** (10.0 μM) for 30 min. In another three groups, cells were pre-treated with 7-nitroindazole (10.0 and 20.0 μM) for 8 h, respectively, and then treated with L-Arg (100.0 μM) for 4 h, followed by staining with **DCI-HA-2** (10.0 μM) for 30 min.

Each cell group was washed with PBS buffer three times (1.0 mL × 3). Confocal imaging experiments were performed on an Olympus FV3000 confocal microscope, and the mean fluorescence intensity was analyzed by Image J software.

1.7 Imaging of HA in PD model cells

For PD model cell imaging, PC-12 cells, SH-SY5Y cells, and BV2 cells were treated with MPP^+ (1.0 and 2.0 mM) for 24 h, 6-OHDA (1.0 and 2.0 mM) for 12 h, and rotenone (5.0 and 10.0 μM) for 1 h, respectively, and then stained with **DCI-HA-2** (10.0 μM) for 30 min.

For HA and H_2S imaging, PC-12 cells were pre-treated with MPP^+ (1.0 and 2.0 mM) for 24 h and then co-stained with **DCI-HA-2** (10.0 μM) and **N-H_2S** (10.0 μM) for 30 min. In nNOS inhibitor groups, cells were pre-treated with 7-nitroindazole (10.0 and 20.0 μM) for 8 h, respectively, and then treated with MPP^+ (2.0 mM) for another 24 h, followed by co-staining with **DCI-HA-2** (10.0 μM) and **N-H_2S** (10.0 μM) for 30 min. In CBS intervention groups, cells were pre-treated with tyrosol (0.5 and 1.0 mM) for 24 h, respectively, and then treated with MPP^+ (2.0 mM) for another 24 h, followed by co-staining with **DCI-HA-2** (10.0 μM) and **N-H_2S** (10.0 μM) for 30 min.

For HA imaging in PD model cells, PC-12 cells were treated with MPP^+ (1.0 and 2.0 mM) for 24 h and subsequently stained with **DCI-HA-2** (10.0 μM) for 30 min. In another two groups, cells were pre-treated with 7-nitroindazole (10.0 and 20.0 μM) for 8 h, respectively, and then treated with MPP^+ (2.0 mM) for 24 h, followed by staining with **DCI-HA-2** (10.0 μM) for 30 min.

After staining, all cell groups were washed with PBS buffer three times (1.0 mL × 3). Confocal imaging experiments were performed on an Olympus FV3000 confocal microscope, and the relative fluorescence intensity was analyzed by Image J software.

1.8 Evaluation of the expression of proteins

PC-12 cells in each group were collected by scraping and lysing with RIPA buffer, and protein concentration was determined with a BCA protein quantification kit. A total of 30.0 μg of protein was separated by 10% SDS-PAGE and transferred onto PVDF membranes. Primary antibodies were diluted as follows: anti-CBS (1:2000, 14787-1-AP, Wuhan Sanying Biotechnology Co., Ltd, China), anti-nNOS (1:500, R1510-28, HUABIO Biotechnology Co., Ltd, China), anti-AMPK (1:1000, ET1608-40, HUABIO Biotechnology Co., Ltd, China), anti- Phospho-AMPK (1:1000, ET1612-72, HUABIO Biotechnology Co., Ltd, China), anti-GAPDH (1:20000, 60004-1-Ig, Wuhan Sanying Biotechnology Co., Ltd, China) and anti-*β*-tubulin (1:5000, 10094-1-AP, Wuhan Sanying Biotechnology Co., Ltd, China). Membranes were incubated with primary antibodies at 4 ℃ overnight.

After washing by 1×Tris-buffered saline with Tween (TBST) for three times (10 min each),

the membranes were further incubated with corresponding horseradish peroxidase-conjugated secondary antibodies diluted by 1×TBST for 2.0 h at room temperature. After that, the membranes were washed three times with 1×TBST and visualized by ChemiDoc Touch Imaging System (Bio-Rad, USA). Band intensities were analyzed by Image Lab software.

1.9 ATP assay

Intracellular ATP levels were determined using an Enhanced ATP Assay Kit (S0027, Beyotime,). Briefly, PC-12 cells were seeded on a 6-well plate with a density of 2×10^5 cells per well and cultured overnight ($n = 3$). Then, the cells were respectively incubated with different treatments as mentioned in Fig. 7D. After that, cells were lysed by 200 μL of lysis buffer. Then, the supernatant was collected and the total ATP levels were calculated on the basis of the chemiluminescence by using a multifunctional microplate reader (Thermo Scientific, USA).

1.10 Animals

C57BL/6 mice (male, 8~10 weeks) were purchased from Hunan SJA Laboratory Animal Co., Ltd (Hunan, China). All animal experiments were carried out in accordance with national guidelines and all procedures were approved by the ethical committees of Central South University (No. 430727211101478756) and Zhejiang University (ZJU20250124).

1.11 Biocompatibility

DCI-HA-2 (200.0 μg/kg) was administered via tail vein injection. The mice were euthanatized after 24 h injection, and main organs (heart, liver, spleen, lung, and kidney) in each group were collected and fixed in 4% paraformaldehyde for 48 h. Various tissue sections were stained with hematoxylin and eosin (H&E) and imaged by Olympus VS200 digital slice scanner.

1.12 Fluorescence imaging of PD model mice

C57BL/6 mice (male, 8~10 weeks) were randomly divided into two groups ($n = 6$): (i) a wild-type group receiving a standard diet for 7 days, and (ii) a PD model group treated with MPTP (25.0 mg/kg, intraperitoneal injection) once daily for 7 consecutive days. Following model establishment, **DCI-HA-2** (200.0 μg/kg) was administered via tail vein injection and fluorescence imaging was performed at 1, 3, 6, 9, and 12 h post-injection using an AniView100 living imaging system.

1.13 Fluorescence imaging of HA in various tissues

After *in vivo* imaging, the mice in each group were euthanized. Major organs, including brain, heart, liver, spleen, lung, and kidney, were collected and washed with PBS buffer three times, and then imaged by AniView100 living imaging system.

1.14 Fluorescence imaging of HA in brain slices

After organ imaging, brain tissues in each group were sectioned into approximately 20 μm thick slices, which were fixed and imaged using an Olympus VS200 digital slice scanner.

1.15 Pharmacokinetic studies

Healthy Sprague-Dawley (SD) rats (male, weighted 180-220 g) were treated with **DCI-HA-2** (200.0 μg/kg) via tail vein injections. Plasma and brain samples were collected at 0.5, 1, 2, 4, 8, and 24 h after post-administration following perfusion. The concentration of **DCI-HA-2** was quantified using LC-MS/MS (AB6500+/EXIONLC ADMP, ESI, C18 1.7 μm 2.1×50 mm, flow rate 0.3 mL/min, mobile phase: 0.1% formic acid in CH_3CN: Methanol = 9:1). Pharmacokinetic parameters were further analyzed, including the peak concentration of (C_{max}), the peak time (T_{max}), the area under the

curve for **DCI-HA-2** levels in the plasma/brain from time zero to 24 h ($AUC_{0\text{-}24h}$), the area under the curve for **DCI-HA-2** levels in the plasma/brain from time zero to ∞ ($AUC_{0\text{-}\infty}$), and elimination half-life ($T_{1/2}$), respectively.

1.16 Biodistribution and clearance study

Healthy C57BL/6 mice (male, 8~10 weeks) were treated with **DCI-HA-2** (200.0 μg/kg) via tail vein injections. After euthanasia, major organs (brain, heart, liver, spleen, lung, and kidney) were collected across a time course (0.5, 1, 2, 4, 8, and 24 h post-administration) and washed with PBS buffer three times, and then imaged by AniView100 living imaging system.

For clearance kinetics, liver and kidney samples were collected at 0.5, 1, 2, 4, 8, and 24 h. Subsequently, quantitative LC-MS/MS was performed to determine the concentration of **DCI-HA-2** in liver and kidney samples.

1.17 Statistical analysis

All statistical analyses were conducted using the GraphPad Prism 9.5. Statistical significance was performed by t-test, with the following criteria: N.S.: no significant difference; * p<0.05; ** p<0.01; *** p<0.001; **** p<0.0001.

2. Results

Table S1. Comparison of fluorescent probes for the detection of HA.

Chemical structure and name	Potential interference	Application	References
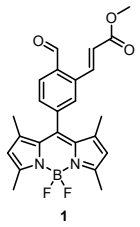 1	Hydrogen sulfide, thiols	Exogenous cell imaging	*Chem. Commun.*, **2017**, *53*, 10441-10443
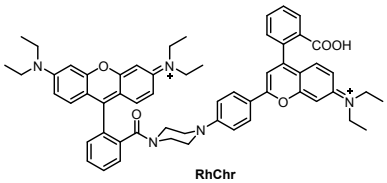 RhChr	Peroxynitrite	Cell and liver tissue imaging	*Anal. Chem.*, **2019**, *91*, 11397-11402
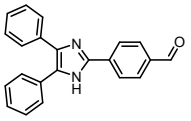 DIB	Hydrogen sulfide, sulfur dioxide derivatives	No	*Org. Biomol. Chem.*, **2020**, *18*, 5963-5971
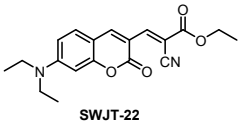 SWJT-22	Thiols	Test strips and cell imaging	*Anal. Chim. Acta.*, **2024**, *1318*, 342941
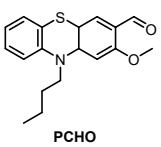 PCHO	Hydrogen sulfide, sulfur dioxide derivatives	Test strips, water samples detection and cell imaging	*Anal. Methods*, **2024**, *16*, 4843-4855

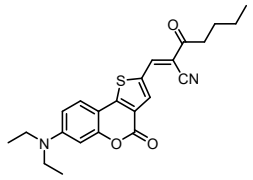 CSO-CY	Thiols	Cell and zebrafish imaging	*Dyes Pigm*. **2026**, *245*, 113218
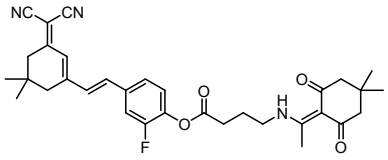 DCI-HA-2	No known interference	Cell imaging, PD model mice imaging, brain tissue imaging, pathway investigation	This work

2.1 General synthesis

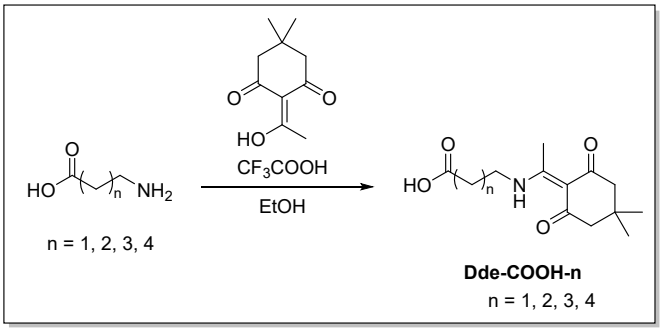

Scheme S1 The synthetic route of **Dde-COOH-n** (*n* = 1-4).

Synthesis of Dde-COOH-1

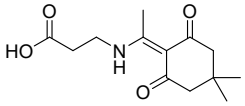

Dde-COOH-1

To a solution of 2-(1-hydroxyethylidene)-5,5-dimethylcyclohexane-1,3-dione (1.53 g, 8.42 mmol) and β-Alanine (1.50 g, 16.84 mmol) in anhydrous ethanol (10.0 mL) was added trifluoroacetic acid (258 μL, 3.37 mmol), and the mixture was refluxed for 18 h. Then, the solvent was removed by rotary evaporator, and 10.0 mL water was added to the residue. Afterward, the mixture was extracted with ethyl acetate (10.0 mL×3) and the organic layer was separated, combined and washed by saturated sodium chloride aqueous solution (15.0 mL×2) and then dried over anhydrous Na_2SO_4. The solvent was removed by rotary evaporator to give a residue, which was purified by column chromatography (silica gel, dichloromethane/methanol = 100/1 to 60/1, v/v) to afford pure **Dde-COOH-1** as a white solid (1.96 g, 7.74 mmol, 92.0%). HRMS(ESI$^+$): calcd. for $C_{13}H_{20}NO$ $[M+H]^+$: 254.1392, found: 254.1443. ^{1}H NMR (600 MHz, CD_3OD) δ 3.75 (t, *J* = 6.4 Hz, 2H), 3.10 (t, *J* = 6.4 Hz, 1H), 2.67 (t, *J* = 6.4 Hz, 2H), 2.58 (s, 3H), 2.53 (t, *J* = 6.4 Hz, 1H), 2.36 (s, 4H), 1.02 (s, 6H). ^{13}C NMR (150 MHz, CD_3OD) δ 198.49, 175.30, 174.12, 173.48, 107.33, 52.01, 48.03, 47.88, 47.74, 47.60, 47.46, 47.31, 47.17, 39.04, 36.22, 33.45, 32.17, 29.60, 26.96, 16.79.

Synthesis of Dde-COOH-2

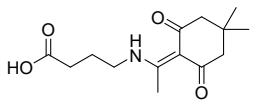

Dde-COOH-2

Dde-COOH-2 was synthesized using a method similar to that for **Dde-COOH-1**, yielding **Dde-COOH-2** as a white solid (2.12 g, 7.93 mmol, 94.9%). HRMS (ESI) calcd. for $C_{14}H_{22}NO_4$ $[M+H]^+$: 268.1549, found: 268.1562. ^{1}H NMR (400 MHz, DMSO-d_6) δ 13.33 – 13.22 (m, 1H), 12.24 (s, 1H), 3.47 – 3.41 (m, 2H), 2.47 (s, 3H), 2.31 (t, J = 7.3 Hz, 2H), 2.27 (s, 4H), 1.79 (p, J = 7.3 Hz, 2H), 0.94 (s, 6H). ^{13}C NMR (100 MHz, DMSO-d_6) δ 196.90, 174.69, 173.31, 107.39, 52.78, 42.80, 40.67, 40.62, 40.41, 40.20, 39.99, 39.78, 39.57, 39.36, 33.54, 30.20, 28.42, 28.33, 22.25, 17.78.

Synthesis of Dde-COOH-3

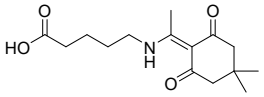

Dde-COOH-3

Dde-COOH-3 was synthesized using a method similar to that for **Dde-COOH-1** as a white solid (2.05 g, 7.29 mmol, 86.1%). HRMS (ESI) calcd. for $C_{15}H_{24}NO_4$ $[M+H]^+$: 282.1705, found: 282.1762. ^{1}H NMR (400 MHz, DMSO-d_6) δ 13.27 (t, J = 5.3 Hz, 1H), 12.07 (s, 1H), 3.43 (q, J = 6.1 Hz, 2H), 2.47 (s, 3H), 2.27 (s, 6H), 1.57 (dq, J = 7.0, 2.7, 1.5 Hz, 4H), 0.94 (s, 6H). ^{13}C NMR (100 MHz, DMSO-d_6) δ 196.90, 174.69, 173.31, 107.39, 52.78, 42.80, 40.67, 40.62, 40.41, 40.20, 39.99, 39.78, 39.57, 39.36, 33.54, 30.20, 28.42, 28.33, 22.25, 17.78.

Synthesis of Dde-COOH-4

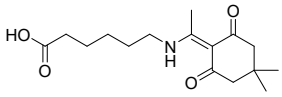

Dde-COOH-4

Dde-COOH-4 was synthesized using a method similar to that for **Dde-COOH-1** as a white solid (2.14 g, 7.24 mmol, 85.3%). HRMS (ESI) calcd. for $C_{16}H_{26}NO_4$ $[M+H]^+$: 296.1862, found: 296.1862. ^{1}H NMR (400 MHz, DMSO-d_6) δ 13.25 (t, J = 5.3 Hz, 1H), 12.03 (s, 1H), 3.41 (td, J = 7.0, 5.3 Hz, 2H), 2.47 (s, 3H), 2.26 (s, 4H), 2.22 (t, J = 7.3 Hz, 2H), 1.55 (dp, J = 17.5, 7.3 Hz, 4H), 1.34 (qd, J = 9.2, 6.1 Hz, 2H), 0.94 (s, 6H). ^{13}C NMR (100 MHz, DMSO-d_6) δ 196.87, 174.82, 173.25, 107.37, 52.79, 42.99, 40.62, 40.41, 40.21, 40.00, 39.79, 39.58, 39.37, 33.97, 30.20, 28.68, 28.33, 26.30, 24.50, 17.76.

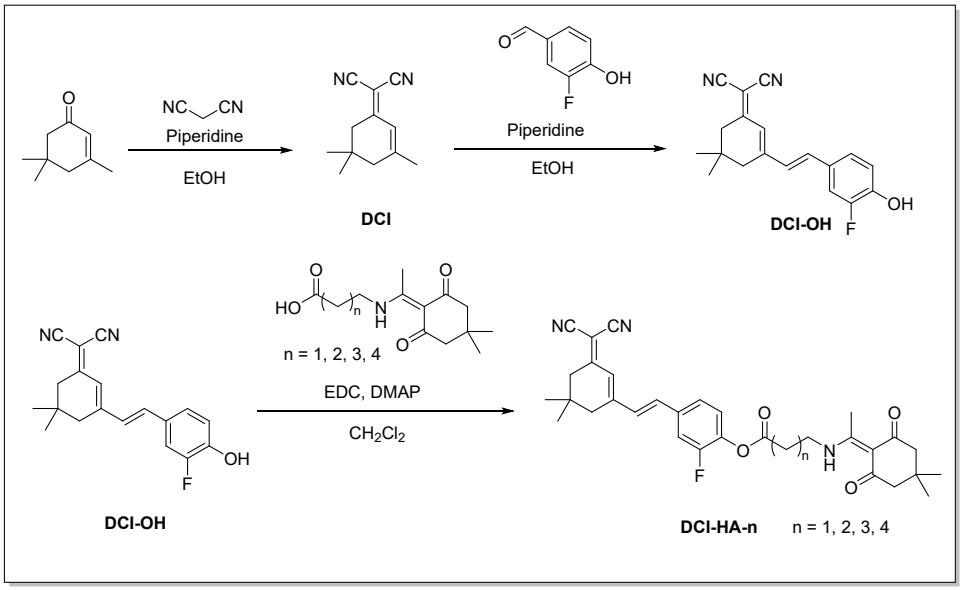

Scheme S2 Synthetic route of **DCI-HA-n** (*n* = 1-4).

Synthesis of DCI

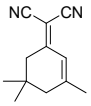

DCI

To a solution of 3,5,5-trimethylcyclohex-2-en-1-one (800.0 mg, 5.78 mmol) and malononitrile (592.0 mg, 6.95 mmol) in anhydrous ethanol (40.0 mL) was added piperidine (100.0 μL, 1.29 mmol), and the mixture was refluxed for 10 h under an argon atmosphere. After cooling to room temperature, the reaction mixture was poured into 60.0 mL water, and a solid precipitated out. The solid was collected by filtration and recrystallized in anhydrous ethanol to afford pure **DCI** as a white solid (861.2 mg, 4.62 mmol, 79.7%). HRMS(ESI$^+$): calcd. for $C_{12}H_{14}N_2Na$ $[M+Na]^+$: 209.1055, found: 209.1075. ^{1}H NMR (500 MHz, $CDCl_3$) δ 6.61 (h, *J* = 1.4 Hz, 1H), 2.50 (s, 2H), 2.17 (dd, *J* = 1.6, 0.9 Hz, 2H), 2.02 (q, *J* = 1.1 Hz, 3H), 1.00 (s, 6H).

Synthesis of DCI-OH

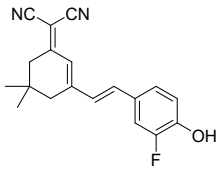

DCI-OH

Under an argon atmosphere, to a solution of 3-fluoro-4-hydroxybenzaldehyde (601.8 mg, 4.30 mmol) and **DCI** (800.0 mg, 4.30 mmol) in anhydrous ethanol (25.0 mL) was added a catalytic amount of piperidine (170.0 μL). The mixture was refluxed for 22 h. The solvent was removed by rotary evaporator, and 10.0 mL water was added to the residue. After removing the solvent, the obtained residue was added ethyl acetate (40.0 mL) and then washed by 10% citric acid aqueous

solution (20.0 mL). The organic layer was separated, combined and washed by saturated sodium chloride aqueous solution (20.0 mL×2) and then dried over anhydrous Na_2SO_4. The solvent was removed by rotary evaporator to give crude product, which was purified by recrystallization in anhydrous ethanol (20.0 mL) to afford pure **DCI-OH** as an orange solid (1.27 g, 4.12 mmol, 96.2%). HRMS (ESI) calcd. for $C_{19}H_{16}FN_2O$ $[M-H]^-$: 307.1247, found: 307.1251. ^1H NMR (400 MHz, Acetone-d_6) δ 7.54 (dd, J = 12.4, 2.1 Hz, 1H), 7.37 (ddd, J = 8.4, 2.1, 1.0 Hz, 1H), 7.24 (s, 2H), 7.03 (t, J = 8.7 Hz, 1H), 6.88 – 6.82 (m, 1H), 2.66 (s, 2H), 2.60 (d, J = 1.3 Hz, 2H), 1.10 (s, 6H).

Synthesis of DCI-HA-1

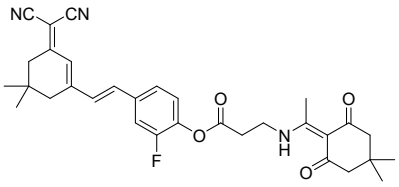

DCI-HA-1

Under an argon atmosphere, **DCI-OH** (200.0 mg, 0.65 mmol), **Dde-COOH-1** (213.6 mg, 0.84 mmol) and 4-dimethylaminopyridine (32.0 mg, 0.26 mmol) were dissolved in dry dichloromethane (20.0 mL) and stirred at room temperature. Subsequently, 1-(3-dimethylaminopropyl)-3-ethylcarbodiimide (223.8 mg, 1.17 mmol) was added in portions, and the reaction was stirred at room temperature for 24 h. Afterward, the mixture was washed by saturated ammonium chloride aqueous solution (20.0 mL). The organic layer was separated, dried over anhydrous Na_2SO_4. The solvent was removed by rotary evaporator to give a residue, which was purified by column chromatography (silica gel, petroleum ether/ ethyl acetate = 1/2 to 1/4, v/v) to give **DCI-HA-1** as a yellow powder (285.1 mg, 0.52 mmol, 80.9%). HRMS (ESI) calcd. for $C_{32}H_{35}FN_3O_4$ $[M+H]^+$: 544.2612, found: 544.2707. ^1H NMR (400 MHz, $CDCl_3$) δ 13.61 (s, 1H), 7.33 – 7.26 (m, 2H), 7.15 (t, J = 7.9 Hz, 1H), 6.94 (d, J = 3.9 Hz, 2H), 6.86 (d, J = 1.4 Hz, 1H), 3.56 (td, J = 7.1, 5.4 Hz, 2H), 2.77 (t, J = 7.1 Hz, 2H), 2.61 (s, 2H), 2.59 (s, 3H), 2.45 (d, J = 1.4 Hz, 2H), 2.38 (s, 4H), 2.13 (p, J = 7.1 Hz, 2H), 1.08 (s, 6H), 1.04 (s, 6H). ^{13}C NMR (100 MHz, $CDCl_3$) δ 198.09, 173.89, 169.78, 169.00, 155.18, 153.19, 152.82, 138.69, 138.59, 135.48, 135.42, 134.46, 134.44, 130.61, 124.43, 124.15, 123.81, 123.79, 115.18, 115.02, 113.25, 112.48, 108.08, 79.73, 77.29, 77.04, 76.78, 52.88, 42.97, 42.14, 39.21, 32.04, 30.72, 30.11, 28.27, 28.01, 24.37, 17.85.

Synthesis of DCI-HA-2

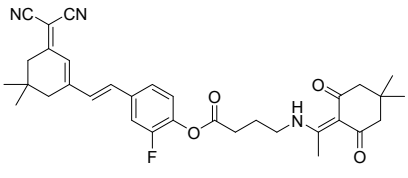

DCI-HA-2

DCI-HA-2 was synthesized in a similar method for **DCI-HA-1** as a yellow solid (318.1 mg, 0.57 mmol, 87.9%). HRMS (ESI) calcd. for $C_{33}H_{37}FN_3O_4$ $[M+H]^+$: 588.2768, found: 588.2754. ^1H NMR (400 MHz, $CDCl_3$) δ 13.61 (s, 1H), 7.33 – 7.26 (m, 2H), 7.15 (t, J = 7.9 Hz, 1H), 6.94 (d, J = 3.9 Hz, 2H), 6.86 (d, J = 1.4 Hz, 1H), 3.56 (td, J = 7.1, 5.4 Hz, 2H), 2.77 (t, J = 7.1 Hz, 2H), 2.61 (s,

2H), 2.59 (s, 3H), 2.45 (d, J = 1.4 Hz, 2H), 2.38 (s, 4H), 2.13 (p, J = 7.1 Hz, 2H), 1.08 (s, 6H), 1.04 (s, 6H). ^{13}C NMR (126 MHz, $CDCl_3$) δ 198.09, 173.89, 169.78, 169.00, 155.18, 153.19, 152.82, 138.69, 138.59, 135.48, 135.42, 134.46, 134.44, 130.61, 124.43, 124.15, 123.81, 123.79, 115.18, 115.02, 113.25, 112.48, 108.08, 79.73, 77.29, 77.04, 76.78, 52.88, 42.97, 42.14, 39.21, 32.04, 30.72, 30.11, 28.27, 28.01, 24.37, 17.85.

Synthesis of DCI-HA-3

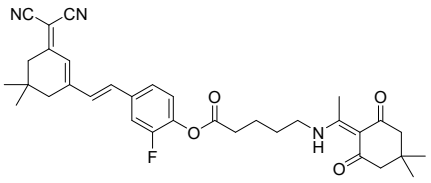

DCI-HA-3

DCI-HA-3 was synthesized in a similar method for **DCI-HA-1** as a yellow solid (322.7 mg, 0.56 mmol, 87.1%). HRMS (ESI) calcd. for $C_{34}H_{39}FN_3O_4$ $[M+H]^+$: 572.2925, found: 572.2935. ^{1}H NMR (600 MHz, $CDCl_3$) δ 13.55 (s, 1H), 7.31 (dd, J = 10.8, 2.0 Hz, 1H), 7.28 (dd, J = 8.4, 2.0 Hz, 1H), 7.15 (t, J = 8.0 Hz, 1H), 6.98 – 6.90 (m, 2H), 6.86 (d, J = 1.6 Hz, 1H), 3.47 (td, J = 6.8, 5.3 Hz, 2H), 2.69 (t, J = 6.9 Hz, 2H), 2.61 (s, 2H), 2.58 (s, 3H), 2.45 (d, J = 1.5 Hz, 2H), 2.38 (s, 4H), 1.92 – 1.87 (m, 2H), 1.84 (qd, J = 6.8, 2.7 Hz, 2H), 1.09 (s, 6H), 1.04 (s, 6H). ^{13}C NMR (150 MHz, DMSO-d_6) δ 173.69, 170.25, 169.03, 152.87, 134.55, 130.52, 124.39, 124.25, 123.78, 115.16, 115.03, 113.28, 112.50, 107.92, 79.69, 77.24, 77.03, 76.81, 52.84, 43.05, 42.98, 39.21, 33.22, 32.06, 30.14, 28.40, 28.27, 28.03, 22.11, 17.97.

Synthesis of DCI-HA-4

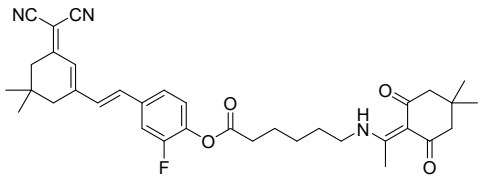

DCI-HA-4

DCI-HA-4 was synthesized in a similar method for **DCI-HA-1** as a yellow solid (341.4 mg, 0.58 mmol, 89.9%). HRMS (ESI) calcd. for $C_{35}H_{41}FN_3O_4$ $[M+H]^+$: 586.3081, found: 586.3076. ^{1}H NMR (500 MHz, $CDCl_3$) δ 13.44 (t, J = 5.2 Hz, 1H), 7.28 – 7.23 (m, 2H), 7.12 (td, J = 8.0, 1.6 Hz, 1H), 6.94 (d, J = 16.1 Hz, 1H), 6.88 (d, J = 16.1 Hz, 1H), 6.81 (s, 1H), 3.42 – 3.36 (m, 2H), 2.61 (td, J = 7.3, 1.7 Hz, 2H), 2.57 (d, J = 2.0 Hz, 2H), 2.53 (d, J = 1.7 Hz, 3H), 2.42 (s, 2H), 2.33 (d, J = 1.9 Hz, 4H), 1.82 – 1.76 (m, 2H), 1.75 – 1.69 (m, 2H), 1.56 – 1.50 (m, 2H), 1.05 (d, J = 1.9 Hz, 6H), 1.00 (d, J = 1.9 Hz, 6H). ^{13}C NMR (125 MHz, $CDCl_3$) δ 173.50, 170.58, 169.06, 155.51, 153.03, 138.97, 138.84, 135.26, 135.20, 134.62, 134.60, 130.46, 128.88, 124.28, 123.82, 123.79, 115.09, 114.90, 113.28, 112.50, 107.85, 79.50, 79.48, 77.49, 77.17, 76.85, 43.15, 42.94, 39.16, 33.49, 31.99, 30.07, 28.72, 28.25, 27.97, 26.97, 26.19, 24.33, 17.87.

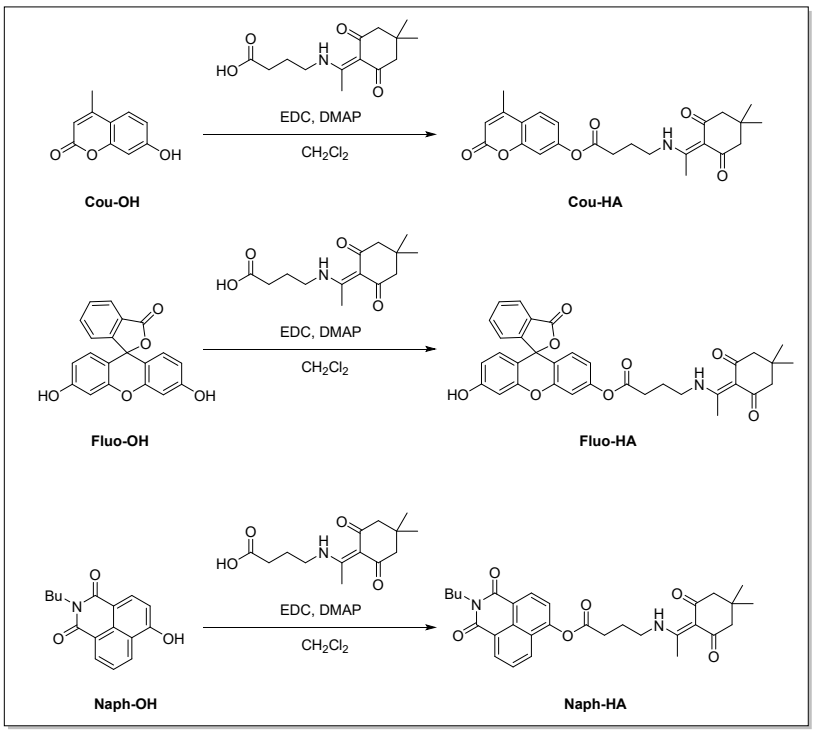

Scheme S3 Synthetic route of **Cou-HA**, **Fluo-HA** and **Naph-HA**.

Synthesis of Cou-HA

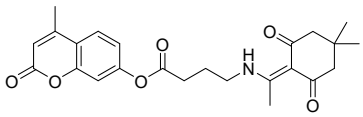

Cou-HA

Using **Cou-OH** as the fluorophore, **Cou-HA** was synthesized in a similar method for **DCI-HA-2** to give a pale white solid (285.2 mg, 0.6728 mmol, 59.0%). HRMS (ESI) calcd. for $C_{24}H_{27}NO_6Na$ $[M+Na]^+$: 448.1736, found: 448.1746. ^1H NMR (500 MHz, $CDCl_3$) δ 13.53 (t, J = 5.4 Hz, 1H), 7.54 (d, J = 8.6 Hz, 1H), 7.03 (d, J = 2.3 Hz, 1H), 7.00 (dd, J = 8.5, 2.3 Hz, 1H), 6.18 (q, J = 1.4 Hz, 1H), 3.50 (td, J = 7.0, 5.4 Hz, 2H), 2.70 (t, J = 7.2 Hz, 2H), 2.52 (s, 3H), 2.36 (d, J = 1.4 Hz, 3H), 2.30 (s, 4H), 2.06 (t, J = 7.1 Hz, 2H), 0.96 (s, 6H). ^{13}C NMR (125 MHz, $CDCl_3$) δ 173.78, 170.34, 160.32, 154.06, 152.76, 151.95, 125.50, 117.90, 114.50, 110.27, 108.01, 77.47, 77.21, 76.96, 42.21, 31.12, 30.03, 28.22, 24.12, 18.67, 17.81.

Synthesis of Fluo-HA

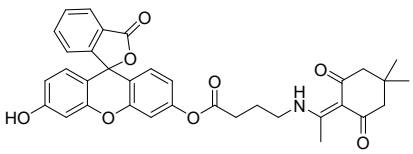

Fluo-HA

Using **Fluo-OH** as the fluorophore, **Fluo-HA** was synthesized in a similar method for **DCI-HA-2** to obtain a light-yellow solid (105.4 mg, 0.18 mmol, 30.5%). HRMS (ESI) calcd. for $C_{34}H_{32}NO_8$ $[M+H]^+$: 582.2128, found: 582.2148. ^1H NMR (400 MHz, $CDCl_3$) δ 13.59 (s, 1H), 8.02 (d, J = 7.4 Hz, 1H), 7.66 (dt, J = 13.5, 7.3 Hz, 2H), 7.17 (d, J = 7.5 Hz, 1H), 7.09 – 7.02 (m, 1H), 6.78 (d, J =

6.8 Hz, 3H), 6.66 (d, *J* = 8.6 Hz, 1H), 6.58 (d, *J* = 8.4 Hz, 1H), 3.60 – 3.52 (m, 2H), 2.73 (s, 2H), 2.60 (s, 3H), 2.39 (s, 4H), 2.12 (s, 2H), 1.04 (s, 6H). ^{13}C NMR (100 MHz, $CDCl_3$) δ 173.08, 169.50, 168.43, 157.40, 150.88, 150.58, 134.17, 128.88, 128.31, 128.12, 125.51, 124.11, 123.03, 116.13, 115.96, 111.74, 109.22, 102.09, 81.58, 76.25, 76.00, 75.75, 41.31, 30.08, 29.13, 28.76, 28.68, 28.30, 27.23, 26.19, 23.17, 21.66, 17.00, 13.10.

Synthesis of Naph-HA

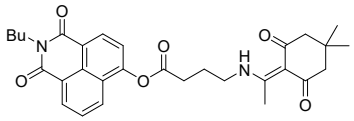

Naph-HA

Using **Naph-OH** as the fluorophore, **Naph-HA** was synthesized in a similar method for **DCI-HA-2** to obtain a pale-yellow solid (185.1 mg, 0.35 mmol, 48.2%). HRMS (ESI) calcd. for $C_{30}H_{35}N_2O_6$ $[M+H]^+$: 519.2495, found: 519.2510. ^{1}H NMR (400 MHz, $CDCl_3$) δ 13.69 (s, 1H), 8.62 (dd, *J* = 11.0, 7.7 Hz, 2H), 8.21 (dd, *J* = 8.5, 1.1 Hz, 1H), 7.79 (dd, *J* = 8.4, 7.3 Hz, 1H), 7.57 (d, *J* = 8.1 Hz, 1H), 4.22 – 4.13 (m, 2H), 3.62 (q, *J* = 6.6 Hz, 2H), 2.96 (t, *J* = 7.2 Hz, 2H), 2.61 (s, 3H), 2.40 (s, 4H), 2.25 – 2.19 (m, 2H), 1.70 (ddt, *J* = 9.3, 7.5, 3.5 Hz, 2H), 1.48 – 1.40 (m, 2H), 1.04 (s, 6H), 0.97 (t, *J* = 7.3 Hz, 3H). ^{13}C NMR (100 MHz, $CDCl_3$) δ 172.91, 169.19, 162.98, 162.41, 150.09, 130.71, 130.65, 128.35, 126.38, 124.02, 122.06, 119.66, 118.31, 107.14, 76.33, 76.01, 75.69, 51.86, 41.17, 39.29, 30.13, 29.17, 29.11, 27.25, 23.19, 19.35, 16.92, 12.82.

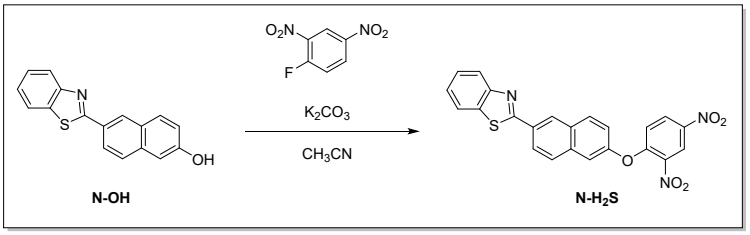

N-OH **N-H$_2$S**

Scheme S4 Synthetic route of **N-H$_2$S**.

Synthesis of N-H$_2$S

N-OH was synthesized according to the literature method.[1]

Under an argon atmosphere, **N-OH** (200.0 mg, 0.72 mmol), K_2CO_3 (150.0 mg, 1.08 mmol) and 2,4-dinitrofluorobenzene (161.1 mg, 0.86 mmol) were dissolved in acetonitrile (10.0 mL) and stirred at 85 ℃ for 18 h. After cooling to room temperature, the solvent was removed by rotary evaporator, and the residue was purified by column chromatography (silica gel, petroleum ether/ ethyl acetate = 2/1 to 1/2, v/v) to give **N-H$_2$S** as a white powder (269.5 mg, 0.61 mmol, 84.2%). HRMS (ESI) calcd. for $C_{23}H_{14}N_3O_5S$ $[M+H]^+$: 444.0654, found: 444.0785. ^{1}H NMR (400 MHz, DMSO-d_6) δ 8.96 (d, *J* = 2.8 Hz, 1H), 8.80 (d, *J* = 1.8 Hz, 1H), 8.48 (dd, *J* = 9.3, 2.8 Hz, 1H), 8.36 (d, *J* = 8.9 Hz, 1H), 8.29 (dd, *J* = 8.6, 1.8 Hz, 1H), 8.20 (dd, *J* = 8.1, 1.3 Hz, 1H), 8.15 – 8.07 (m, 2H), 7.89 (d, *J* = 2.5 Hz, 1H), 7.65 – 7.54 (m, 2H), 7.50 (ddd, *J* = 8.3, 7.2, 1.2 Hz, 1H), 7.36 (d, *J* = 9.3 Hz, 1H). ^{13}C NMR (100 MHz, DMSO-d_6) δ 167.54, 154.94, 154.10, 153.50, 142.35, 140.24, 135.65, 135.09, 132.63, 131.29, 130.89, 130.22, 129.25, 127.86, 127.82, 127.29, 127.03, 126.20, 125.62, 125.53, 123.41, 122.95, 122.46, 121.40, 120.79, 117.07.

Reference

[1] Xiao-Hong Zhou, Yu-Ren Jiang, Xiong-Jie Zhao, Dong Guo, *Talanta*, 2016, **160**, 470-474.

2.2 Time-dependent responses of DCI-HA-n towards HA

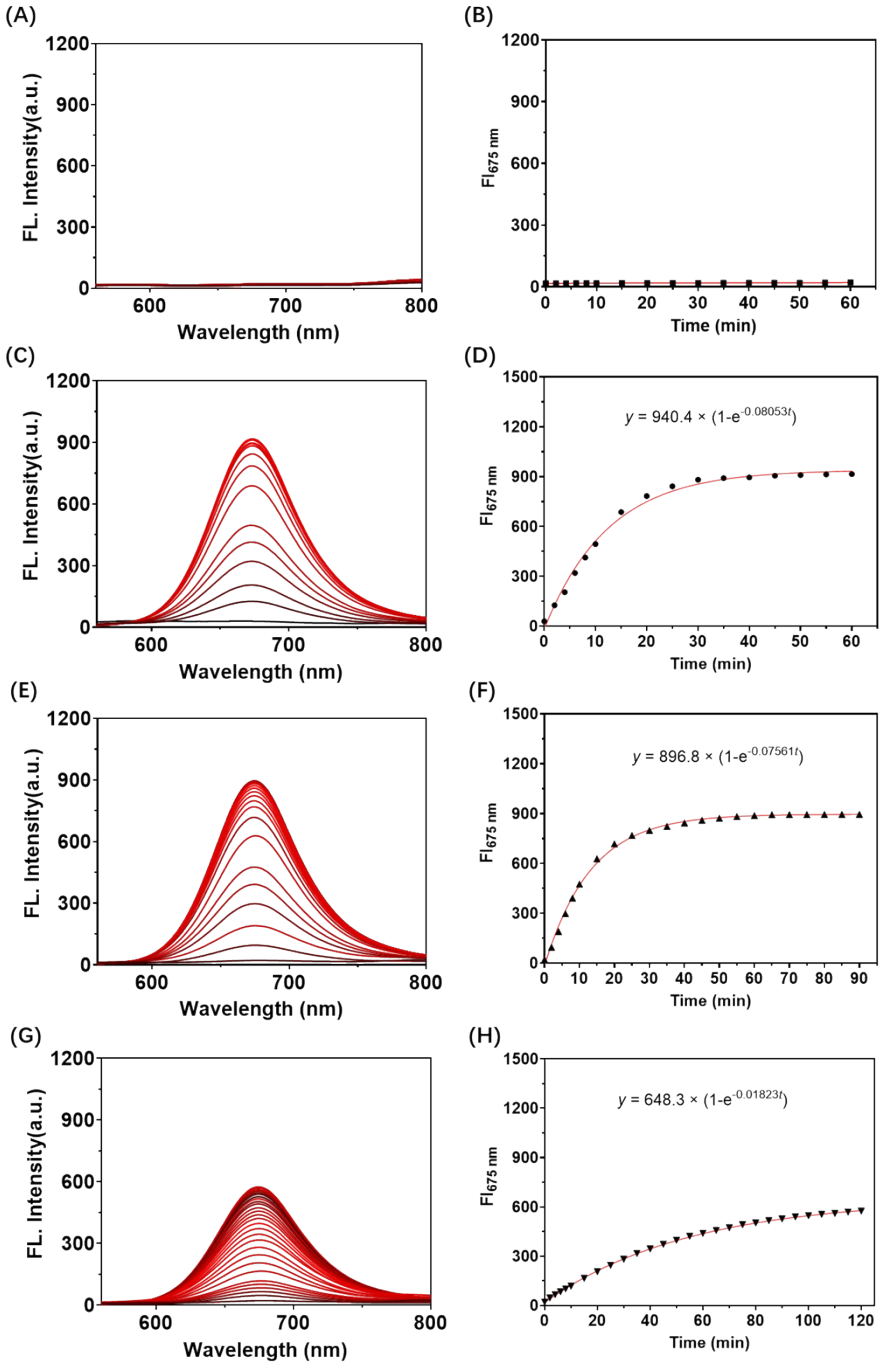

Fig. S1 Time-dependent fluorescence spectra of 10.0 μM of (A) **DCI-HA-1**, (C) **DCI-HA-2**, (E) **DCI-HA-3**, and (G) **DCI-HA-4** in the presence of HA (10.0 μM) in PBS (10 mM, pH = 7.4, 1% DMSO), respectively. *Pseudo-first-order* kinetic curves of fluorescence intensity at 675 nm of (B) **DCI-HA-1**, (D) **DCI-HA-2**, (F) **DCI-HA-3** and (H) **DCI-HA-4** towards HA, respectively. λ_{ex} = 480 nm.

2.3 Response mechanism study

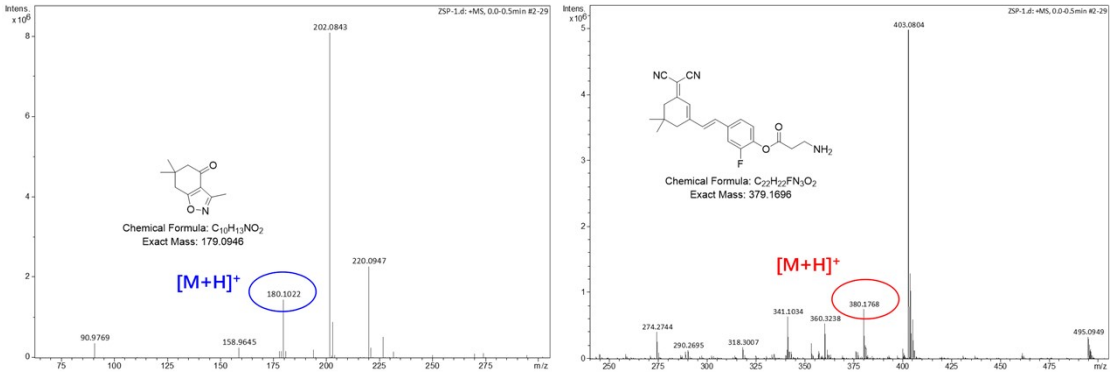

Fig. S2 HRMS spectra of the mixture of **DCI-HA-1** (10.0 μM) with HA (20.0 μM).

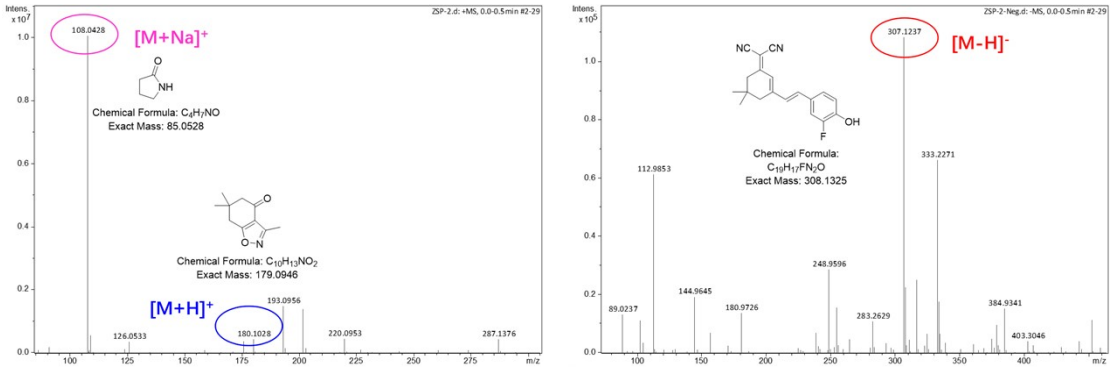

Fig. S3 HRMS spectra of the mixture of **DCI-HA-2** (10.0 μM) with HA (20.0 μM).

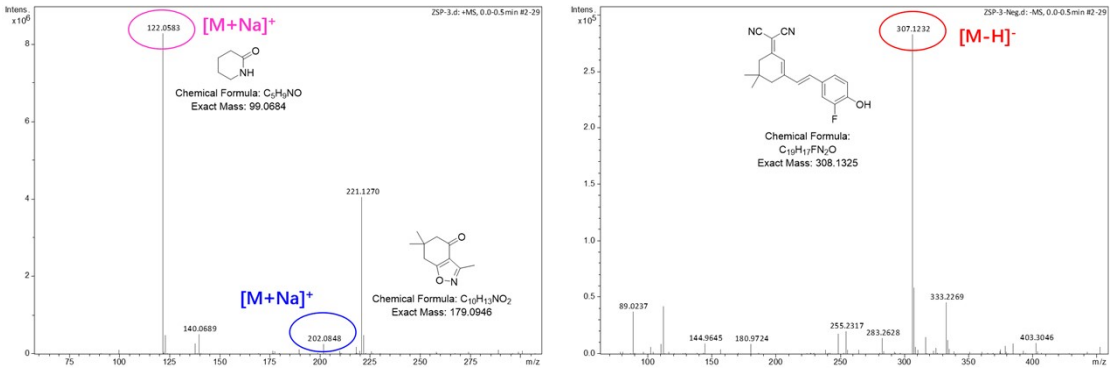

Fig. S4 HRMS spectra of the mixture of **DCI-HA-3** (10.0 μM) with HA (20.0 μM).

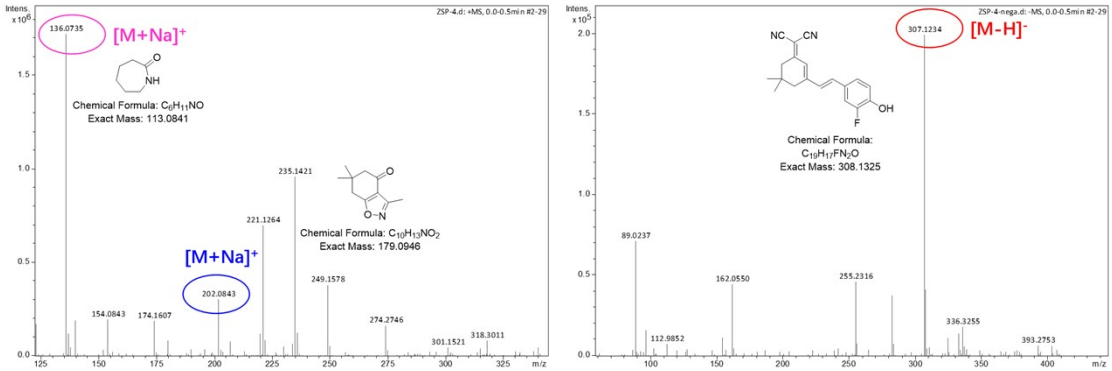

Fig. S5 HRMS spectra of the mixture of **DCI-HA-4** (10.0 μM) with HA (20.0 μM).

2.4 Anti-interference test

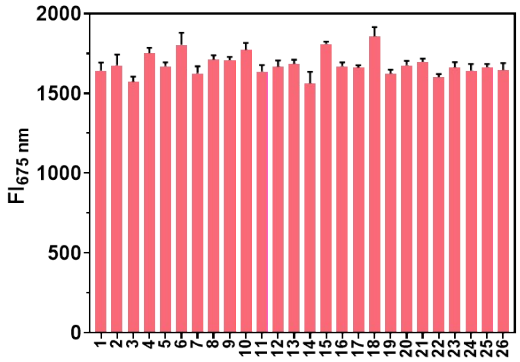

Fig. S6 Fluorescence intensity at 675 nm of **DCI-HA-2** (10.0 μM) towards HA (20.0 μM) in the presence of various bioactive species (1~26: Blank, Fe^{3+}, Fe^{2+}, Zn^{2+}, Mg^{2+}, Cu^{2+}, Ca^{2+}, HSO_3^-, SO_3^{2-}, $S_2O_3^{2-}$, S_2^-, H_2O_2, ·OH, $O_2^{\cdot-}$, HOCl, NO_2^-, NO_3^-, $ONOO^-$, HNO, NO, Cys, Hcy, GSH, GSSG, L-arginine and HA; other species at 20.0 μM, GSH at 1.0 mM.

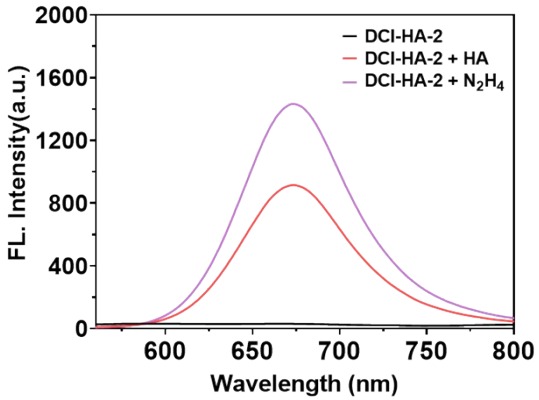

Fig. S7 Fluorescence spectra of **DCI-HA-2** (black line), **DCI-HA-2** + 20.0 μM HA (red lines) and **DCI-HA-2** + 20.0 μM N_2H_4 (purple line). Probe concentration: 10.0 μM. λ_{ex} = 480 nm. Test media: PBS buffer (pH = 7.40, 10 mM) with 1% DMSO.

2.4 Absorption spectra of Cou-HA, Fluo-HA and Naph-HA with and without HA

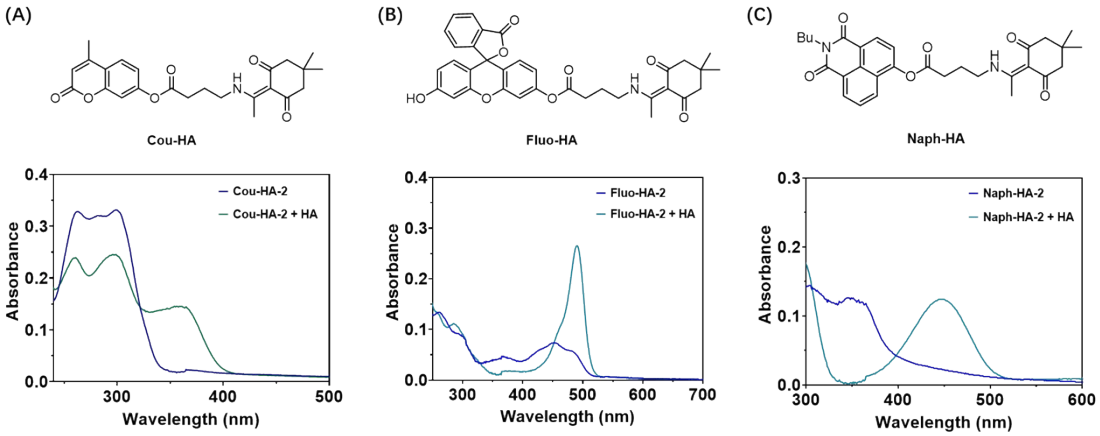

Fig. S8 Chemical structures and absorption spectra of 10.0 μM of each probe before and after adding HA (10.0 μM): (A) **Cou-HA**, (B) **Fluo-HA**, and (C) **Naph-HA**.

2.5 Selectivity of Cou-HA, Fluo-HA and Naph-HA towards HA

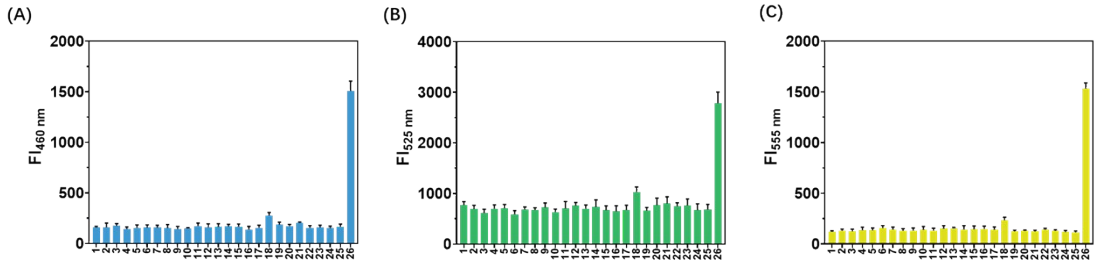

Fig. S9 Fluorescence responses of (A) **Cou-HA**, (B) **Fluo-HA**, and (C) **Naph-HA** towards various bioactive substances (1~26: blank, Fe^{3+}, Fe^{2+}, Zn^{2+}, Mg^{2+}, Cu^{2+}, Ca^{2+}, HSO_3^-, SO_3^{2-}, $S_2O_3^{2-}$, S_2^-, H_2O_2, ·OH, $O_2^{\cdot-}$, HOCl, NO_2^-, NO_3^-, $ONOO^-$, HNO, NO, Cys, Hcy, GSH, GSSG, L-arginine, and HA; other species at 20.0 μM, GSH at 1.0 mM). Data are presented as mean ± SD, n = 3.

2.6 Anti-interference evaluation of Cou-HA, Fluo-HA and Naph-HA

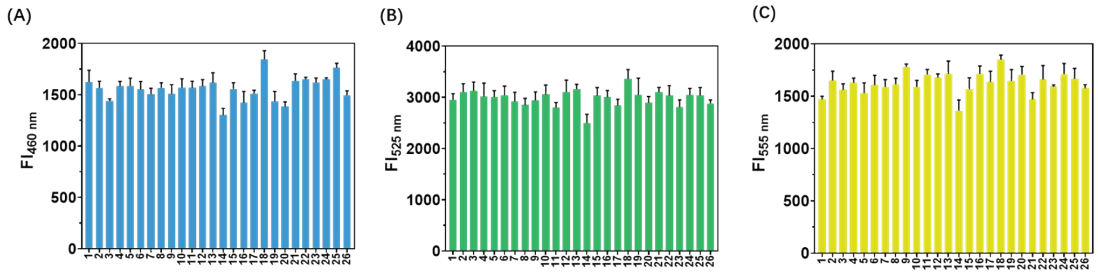

Fig. S10 Fluorescence responses of (A) **Cou-HA**, (B) **Fluo-HA**, and (C) **Naph-HA** towards HA (20.0 μM) in the presence of various bioactive substances (1~26: blank, Fe^{3+}, Fe^{2+}, Zn^{2+}, Mg^{2+}, Cu^{2+}, Ca^{2+}, HSO_3^-, SO_3^{2-}, $S_2O_3^{2-}$, S_2^-, H_2O_2, ·OH, $O_2^{\cdot-}$, HOCl, NO_2^-, NO_3^-, $ONOO^-$, HNO, NO, Cys, Hcy, GSH, GSSG, L-arginine, and HA; other species at 20.0 μM, GSH at 1.0 mM). Data are presented as mean ± SD, n = 3.

2.7 Photostability of Cou-HA, Fluo-HA, Naph-HA and DCI-HA-2

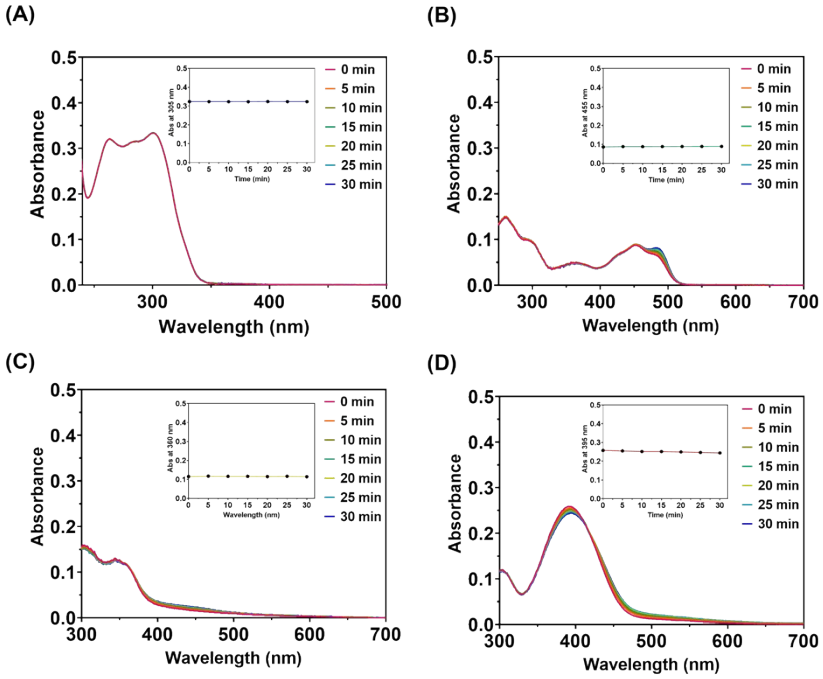

Fig. S11 UV–vis absorption spectra of (A) **Cou-HA**, (B) **Fluo-HA**, (C) **Naph-HA**, and (D) **DCI-HA-2** in PBS buffer (10.0 μM, pH = 7.40) under LED irradiation. Insets: the relative changes in absorbance at the corresponding absorption maximum as a function of irradiation time. Irradiation wavelengths: 300-310 nm for **Cou-HA**, 440-450 nm for **Fluo-HA**, 350-360 nm for **Naph-HA**, and 390-400 nm for **DCI-HA-2**; light intensity: 20 mW/cm^2.

2.8 Cytotoxicity assay

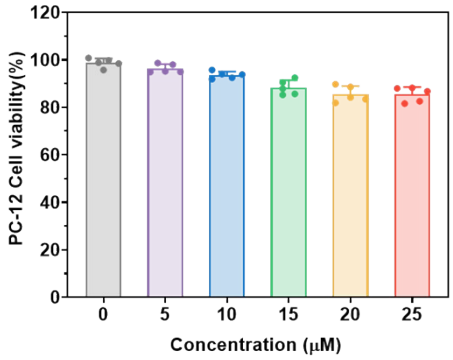

Fig. S12 Cell viabilities of PC-cells treated with different concentrations of **DCI-HA-2** (0, 5.0, 10.0, 15.0, 20.0 and 25.0 μM) for 24 h. Data are expressed as mean ± SD, n = 5.

2.9 Biocompatibility assay

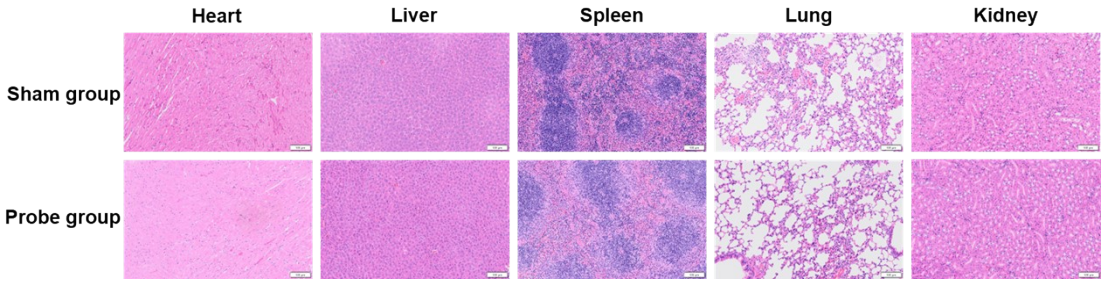

Fig. S13 H&E staining of main organ sections (heart, liver, spleen, lung, and kidney) from the Sham (saline) and probe (**DCI-HA-2**) groups, respectively. Scale bar: 100 μm.

2.10 Fluorescence imaging of HA change in PD model cells

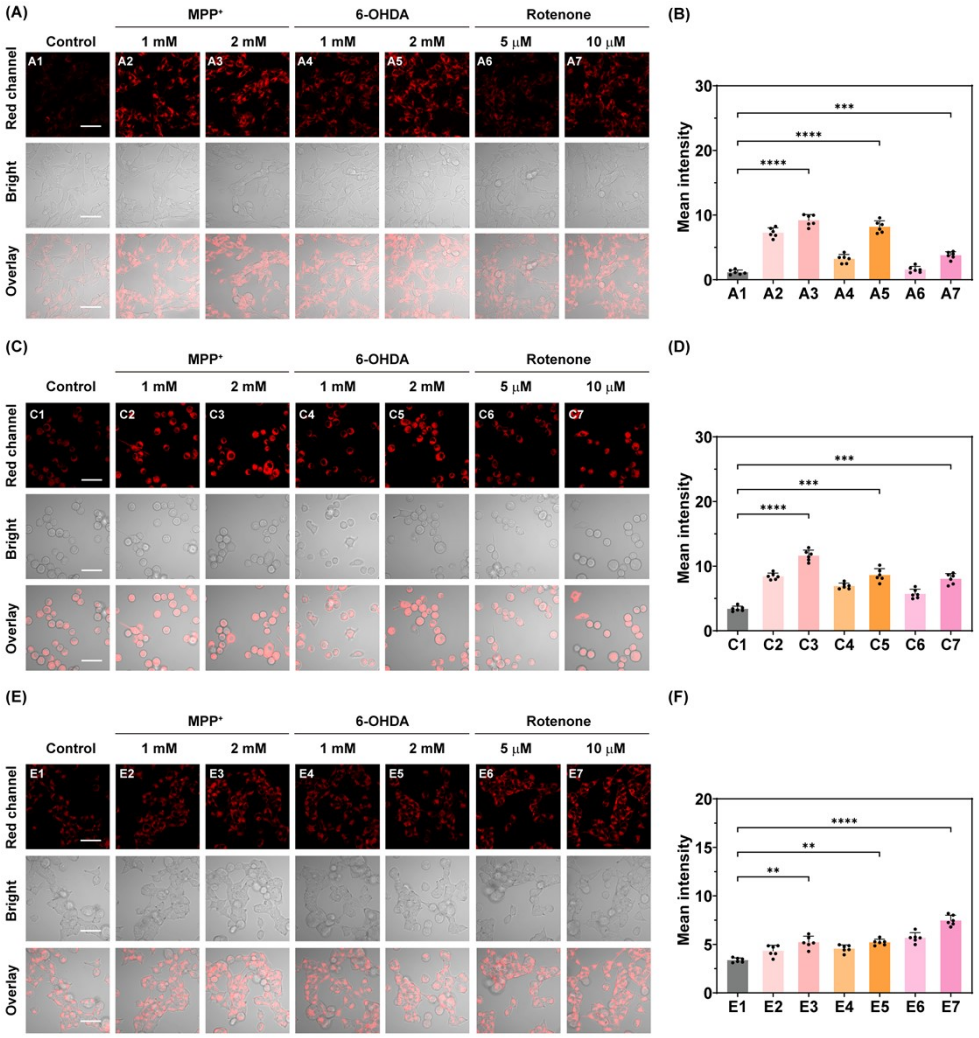

Fig. S14 Fluorescence imaging (A, C, E) and quantification (B, D, F) of cells after different neurotoxin pre-treatments followed by incubation with **DCI-HA-2** (10.0 μM) for 30.0 min. (A, B) SH-SY5Y cells; (C, D) BV2 cells; (D, E) HEK293T cells. Treatment conditions: control; MPP^+ (1.00 or 2.00 mM, for 24 h); 6-OHDA (1.00 or 2.00 mM, for 12 h); rotenone (5.00 or 10.00 μM, 1 h). λ_{ex} = 488 nm, λ_{em} = 620-720 nm. Scale bar = 50.0 μm. Error bars represent SD, n = 6. **** p<0.0001, *** p<0.001, ** p<0.01.

2.11 In vivo fluorescence imaging of HA in mice

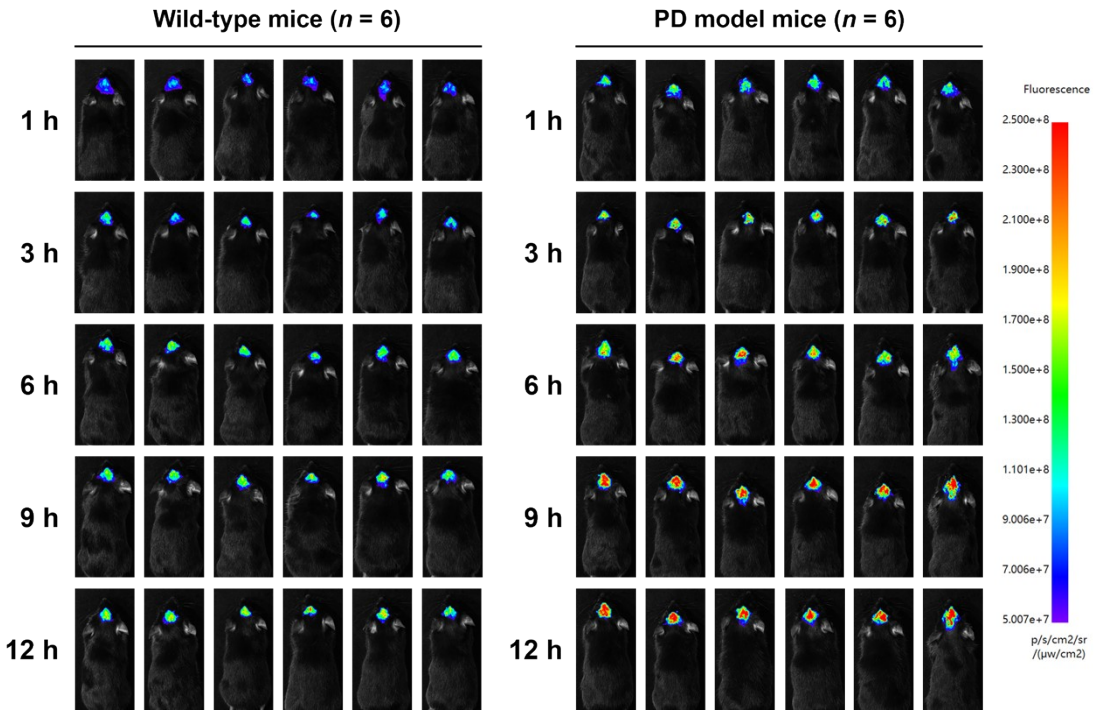

Fig. S15 Fluorescence imaging of HA in wild-type and PD model mice after tail vein injection of **DCI-HA-2** (200 μg/kg), n = 6. λ_{ex} = 488 nm, λ_{em} = 620~720 nm.

2.12 Fluorescence imaging of HA in brain

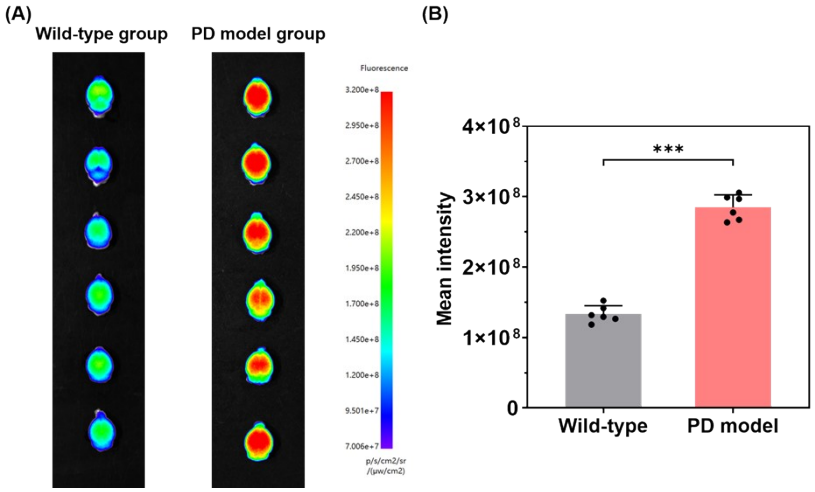

Fig. S16 (A) Fluorescence images of brain tissues collected from each group of mice. (B) Statistical analysis of relative fluorescence intensity in panel (A). λ_{ex} = 488 nm, λ_{em} = 620~720 nm. Error bars represent SD, n = 6. *** p<0.001.

2.13 Fluorescence imaging of main organs

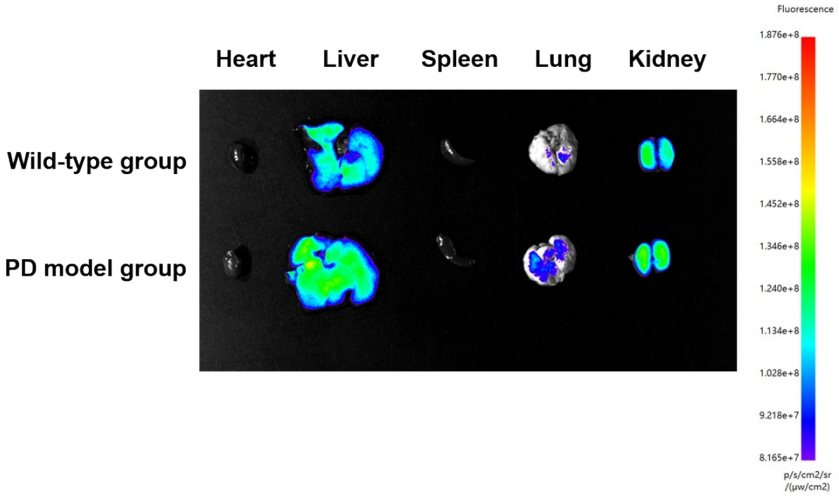

Fig. S17 Fluorescence images of main organs (heart, liver, spleen, lung, and kidney) from mice of each group after intravenous injection of **DCI-HA-2** (200.0 μg/kg). λ_{ex} = 488 nm, λ_{em} = 650~750 nm.

2.14 Pharmacokinetic study of DCI-HA-2

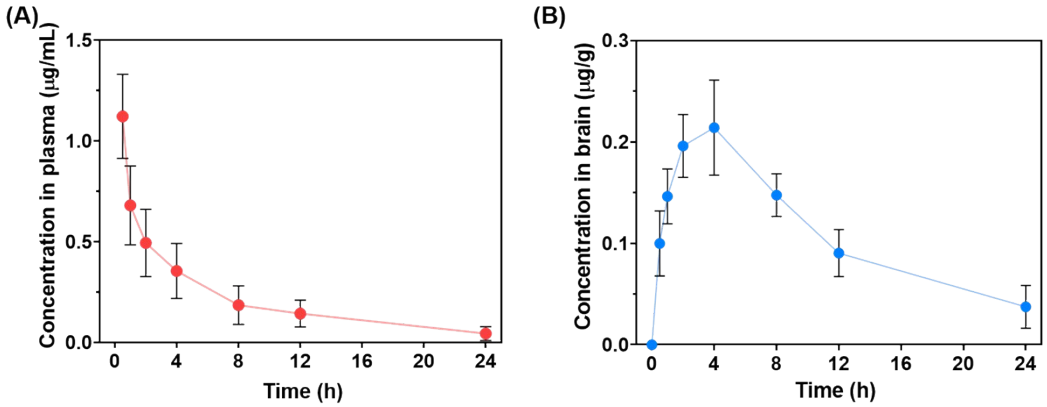

Fig. S18 Pharmacokinetic studies of **DCI-HA-2** in the plasma (A) and brain (B) of mice (n = 3).

Table S2. Pharmacokinetic parameters of **DCI-HA-2** in in the plasma (A) and brain (B) of mice (n = 3).

Sample matrix	C_{max}	T_{max}	$AUC_{0\text{-}24\ h}$	$AUC_{0\text{-}\infty}$	$T_{1/2}$
Plasma	1.122 μg/mL	0.5 h	5.024 μg·h/mL	5.472 μg·h/mL	5.34 h
Brain	0.214 μg/g	4 h	2.632 μg·h/g	3.142 μg·h/g	9.44 h

2.15 Biodistribution and clearance kinetics of DCI-HA-2

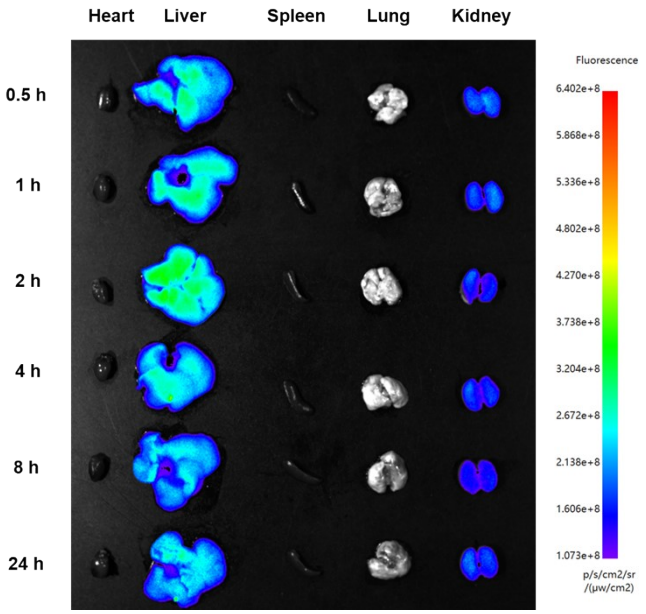

Fig. S19 Fluorescence images of representative major organs of mice at different time points. λ_{ex} = 488 nm, λ_{em} = 650~750 nm.

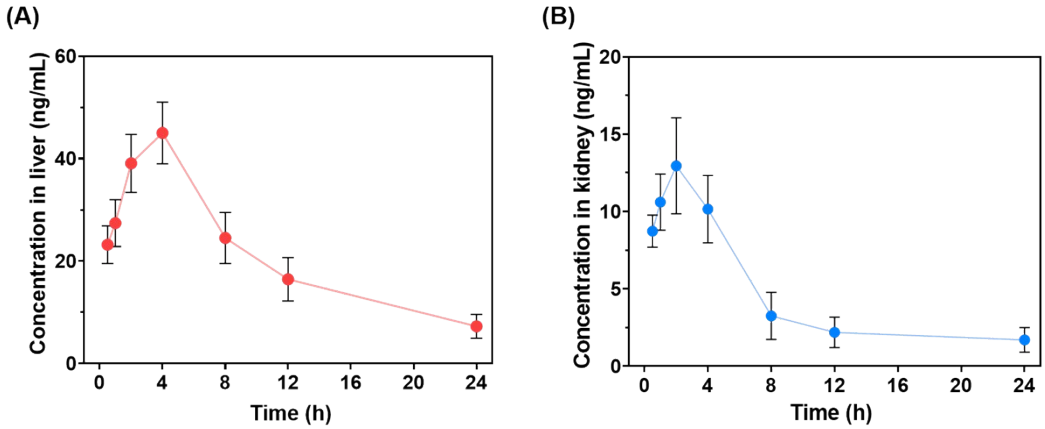

Fig. S20 Clearance kinetics of **DCI-HA-2** in liver and kidney of mice (n = 3).

Table S3. Pharmacokinetic parameters of **DCI-HA-2** in the plasma and brain of mice (n = 3).

Sample matrix	$AUC_{0-\infty}$	*Clearance rate (CL)*
Liver	0.598 mg·h/L	1.11 mL/min
Kidney	0.181 mg·h/L	3.68 mL/min

2.16 Proteomic results of control group, PD cells and 7-nitroindazole-pretreated PD cells

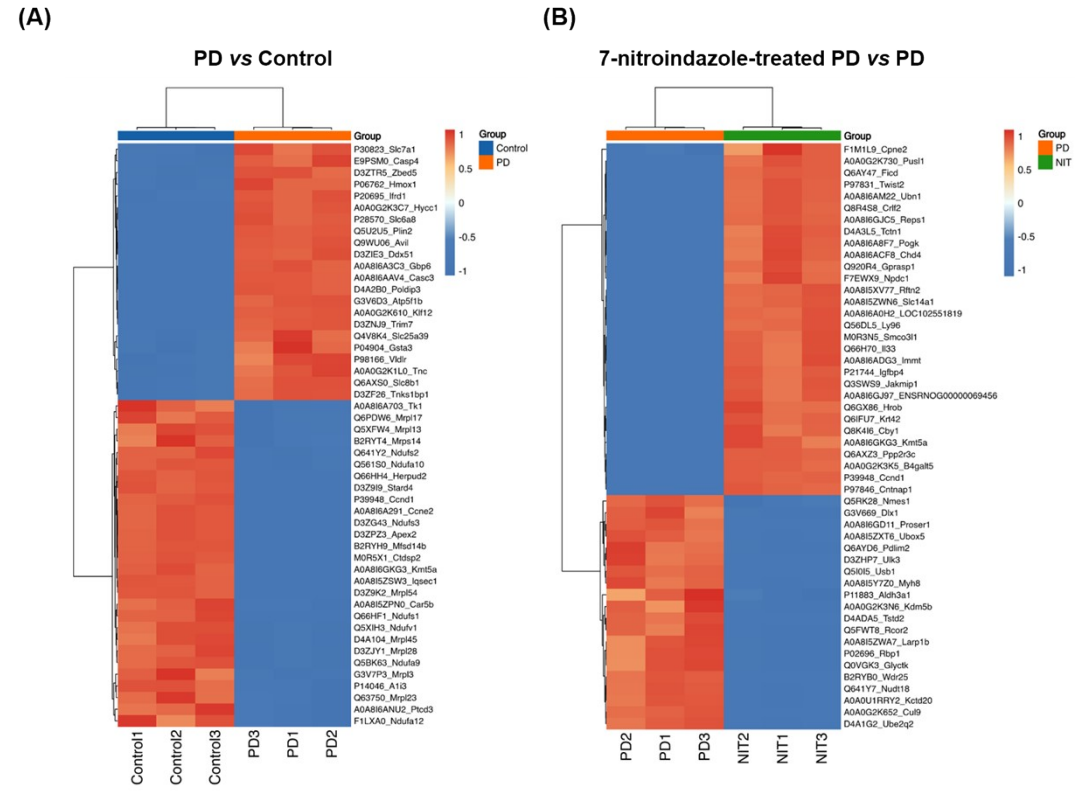

Fig. S21 Heatmap of differential expression proteins in (A) PD group *vs* control group, and (B) 7-nitroindazole-treated PD group *vs* PD group. $n = 3$, $p < 0.05$.

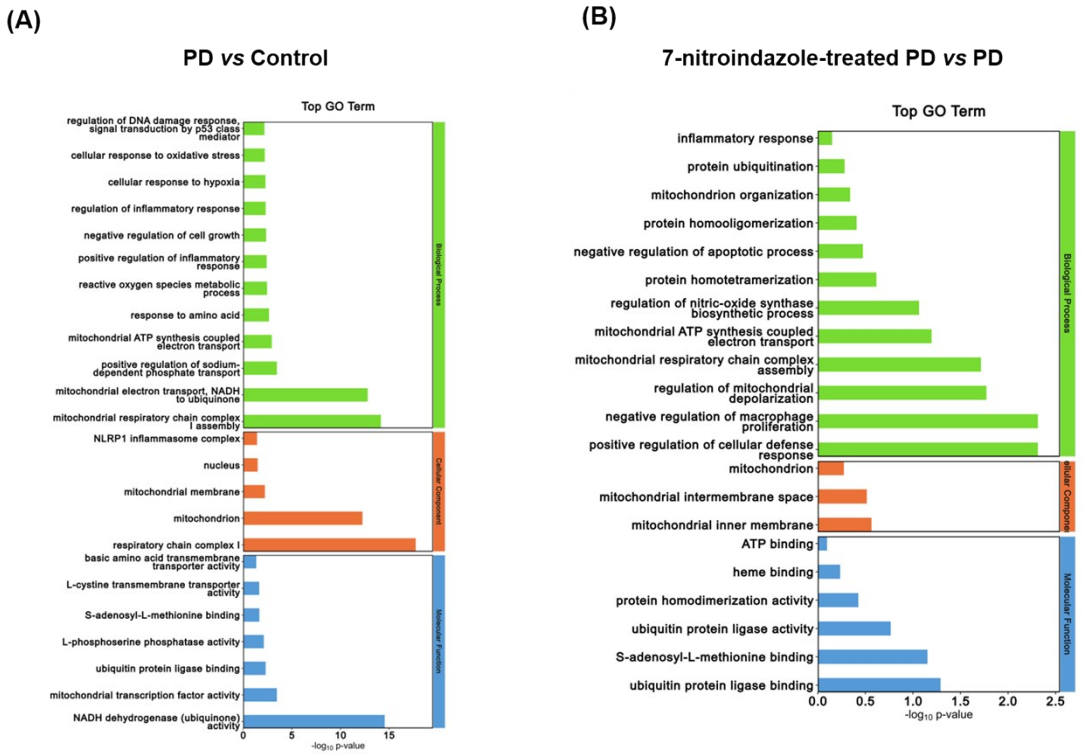

Fig. S22 Gene Ontology (GO) enrichment analysis of differential expression proteins in (A) PD group *vs* control group, and (B) 7-nitroindazole-treated PD group *vs* PD group.

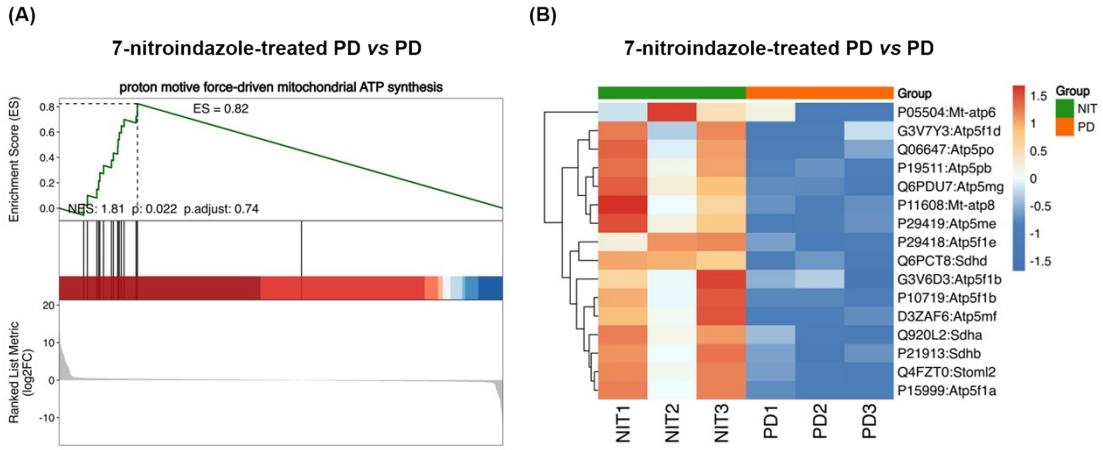

Fig. S23 (A) Gene set enrichment analysis of mitochondrial ATP synthesis between the 7-nitroindazole-treated PD group *vs* PD group. (B) Heatmap of differential expression proteins in (A). $n = 3$.

2.17 Western blot raw gel images

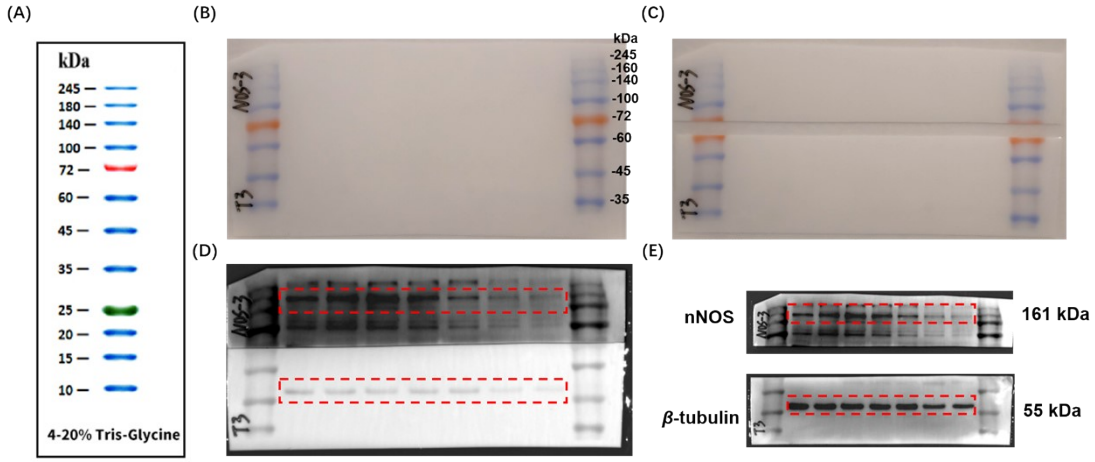

Fig. S24 Raw gel images of nNOS and *β*-tubulin, corresponding to the red dotted box in Fig. 6F.

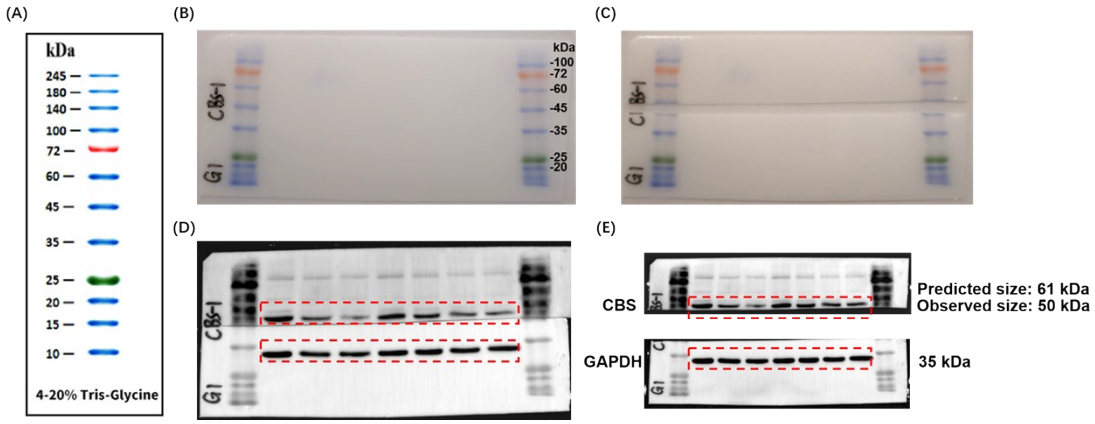

Fig. S25 Raw gel images of CBS and GAPDH, corresponding to the red dotted box in Fig. 6F.

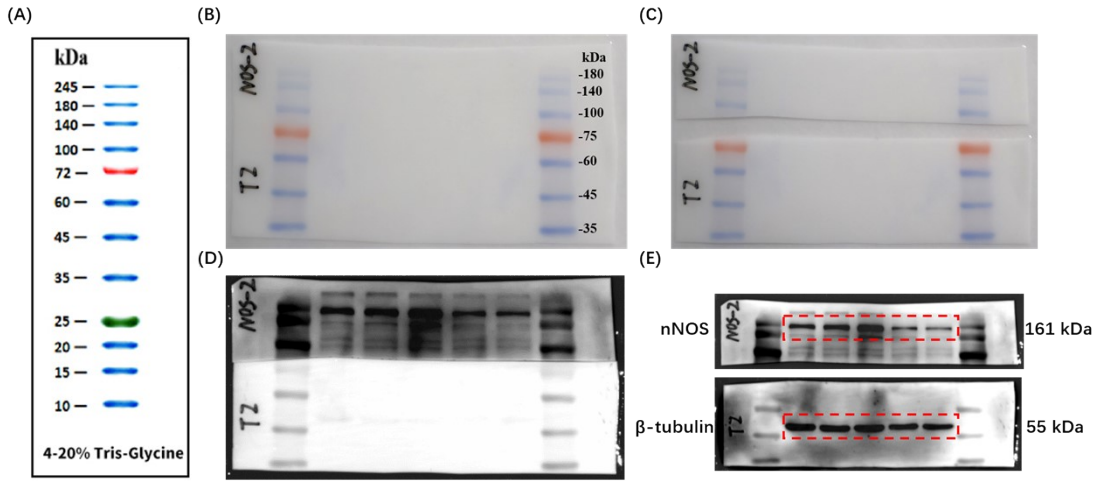

Fig. S26 Raw gel images of nNOS and *β*-tubulin, corresponding to the red dotted box in Fig. 7G.

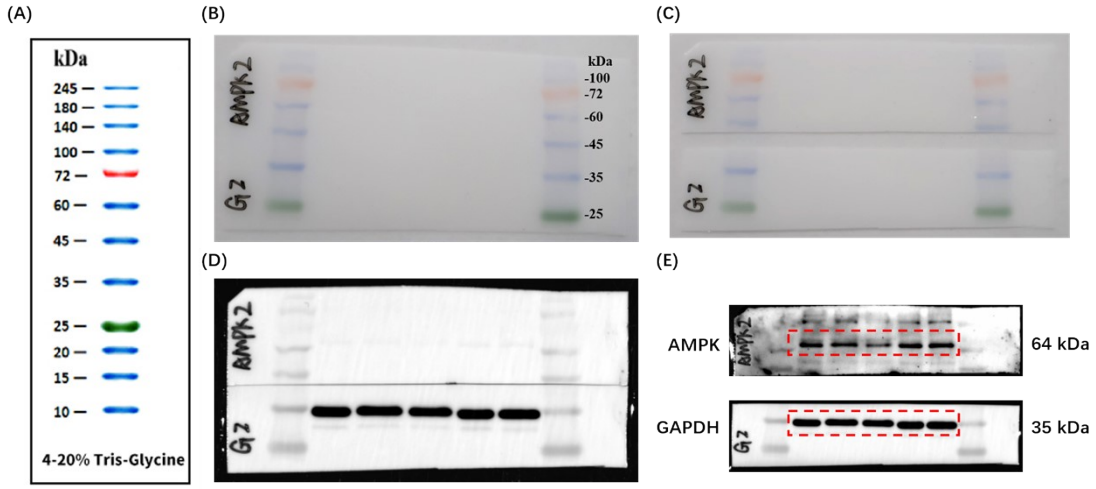

Fig. S27 Raw gel images of AMPK and GAPDH, corresponding to the red dotted box in Fig. 7G.

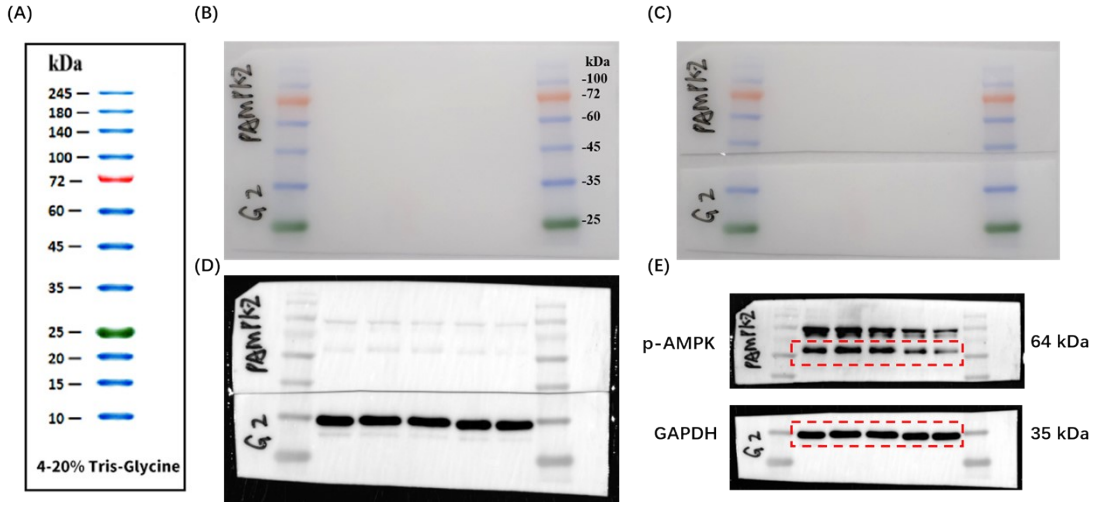

Fig. S28 Raw gel images of p-AMPK and GAPDH, corresponding to the red dotted box in Fig. 7G.

2.18 NMR and HRMS spectral characterization

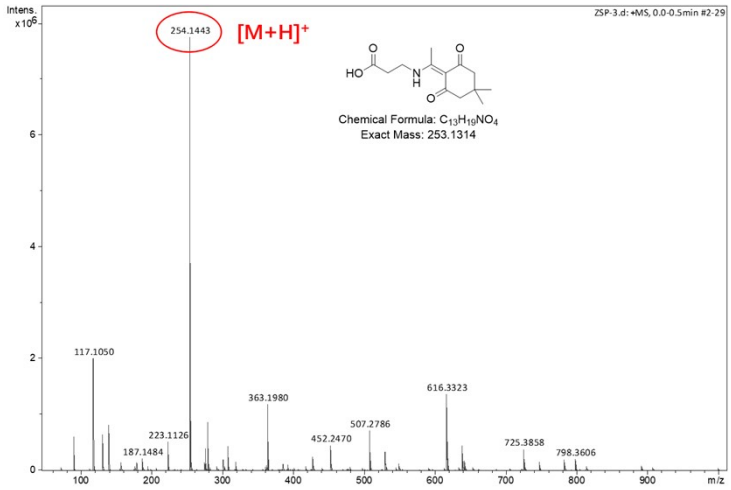

Fig. S29 HRMS spectrum of **Dde-COOH-1**.

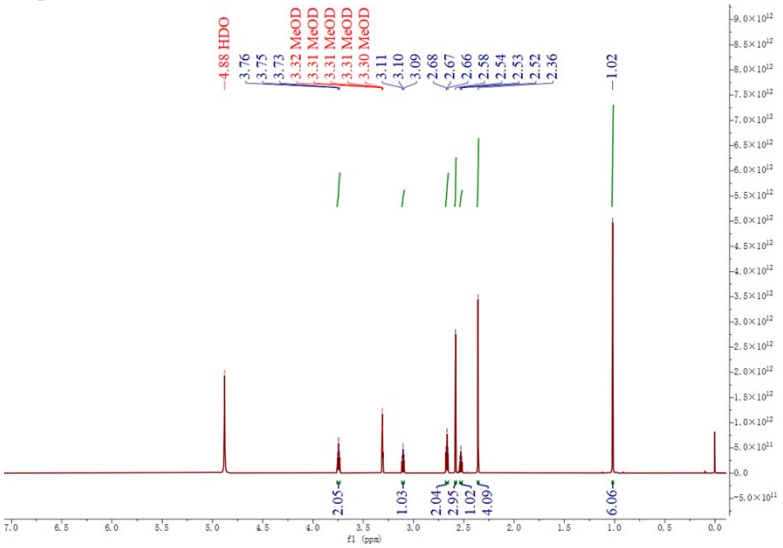

Fig. S30 ^{1}H NMR spectrum of **Dde-COOH-1** in CD_3OD.

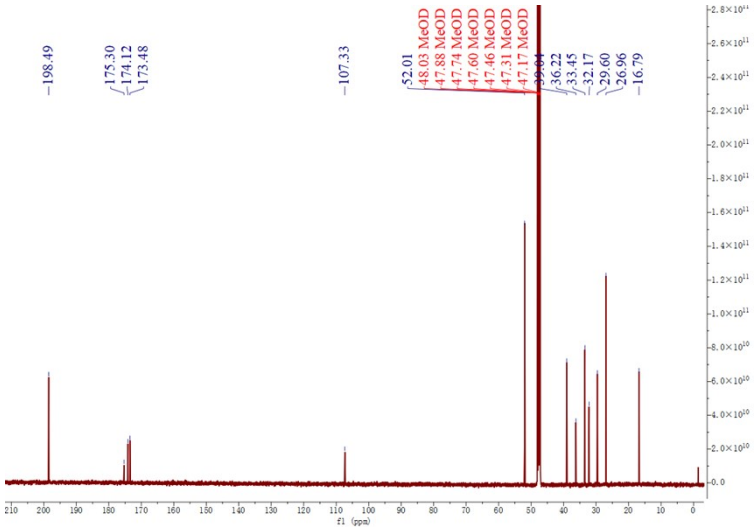

Fig. S31 ^{13}C NMR spectrum of **Dde-COOH-1** in CD_3OD.

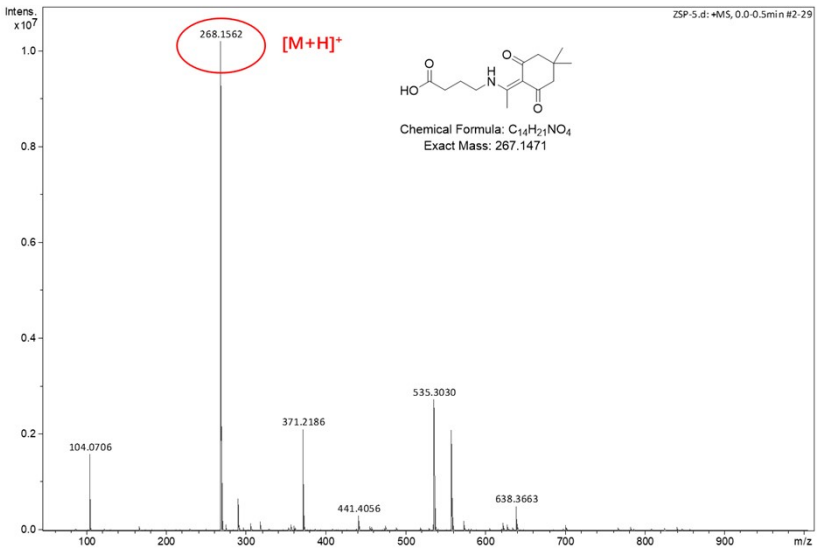

Fig. S32 HRMS spectrum of **Dde-COOH-2**.

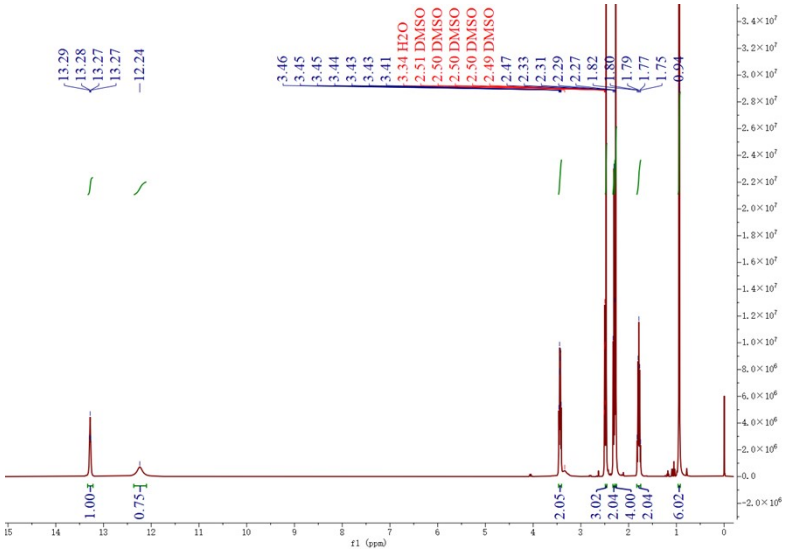

Fig. S33 ^{1}H NMR spectrum of **Dde-COOH-2** in DMSO-d_6.

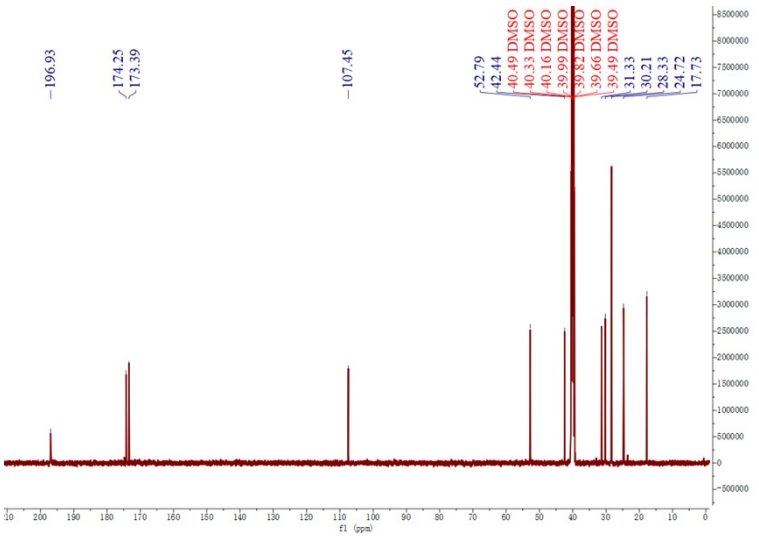

Fig. S34 ^{13}C NMR spectrum of **Dde-COOH-2** in DMSO-d_6.

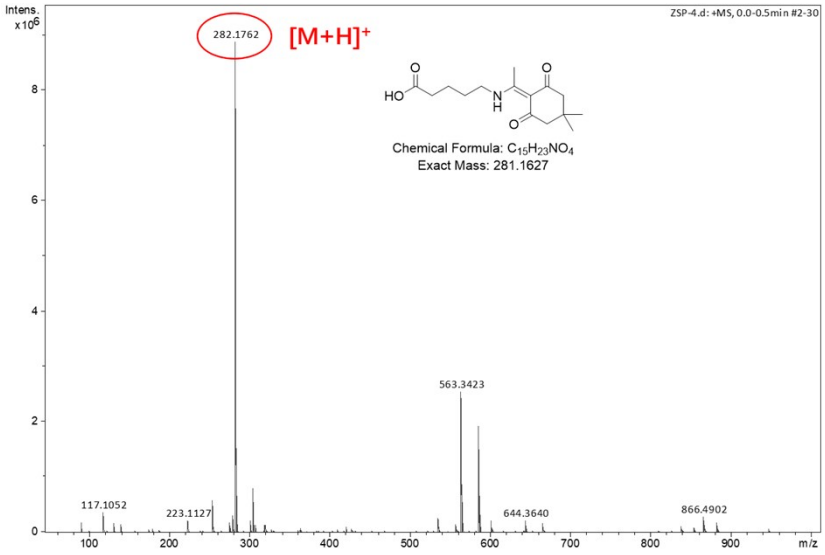

Fig. S35 HRMS spectrum of **Dde-COOH-3**.

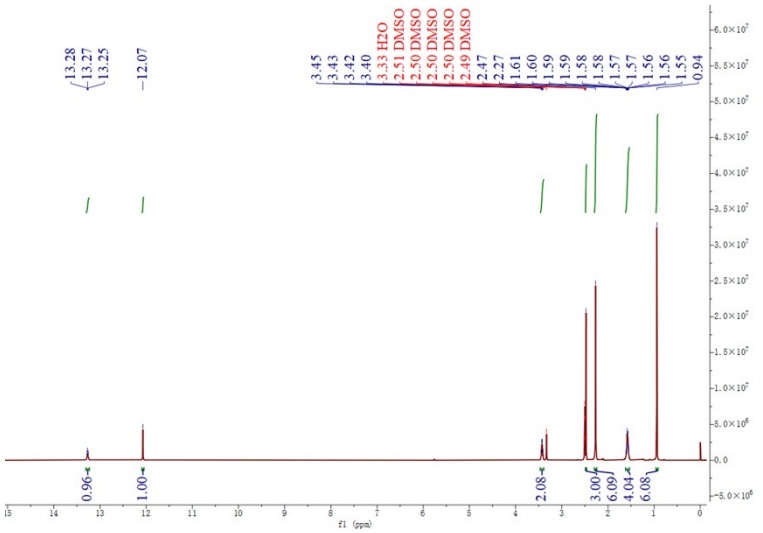

Fig. S36 ^{1}H NMR spectrum of **Dde-COOH-3** in DMSO-d_6.

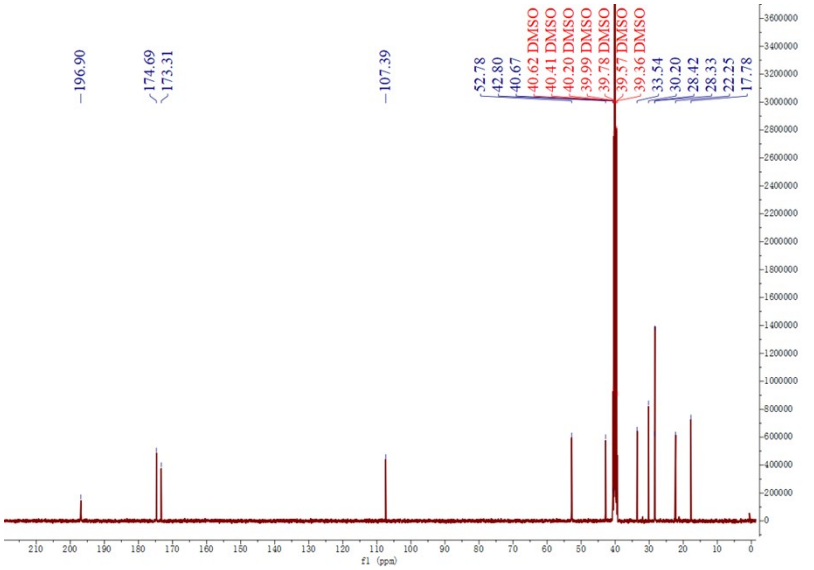

Fig. S37 ^{13}C NMR spectrum of **Dde-COOH-3** in DMSO-d_6.

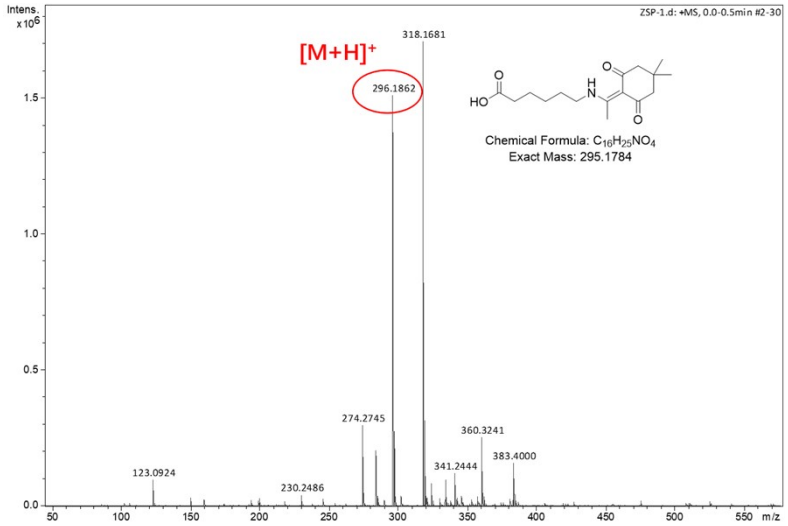

Fig. S38 HRMS spectrum of **Dde-COOH-4**.

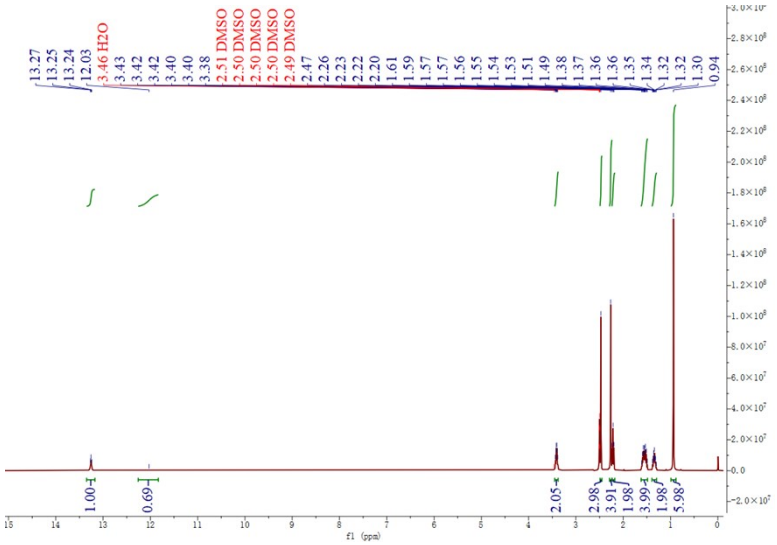

Fig. S39 ^{1}H NMR spectrum of **Dde-COOH-4** in DMSO-d_6.

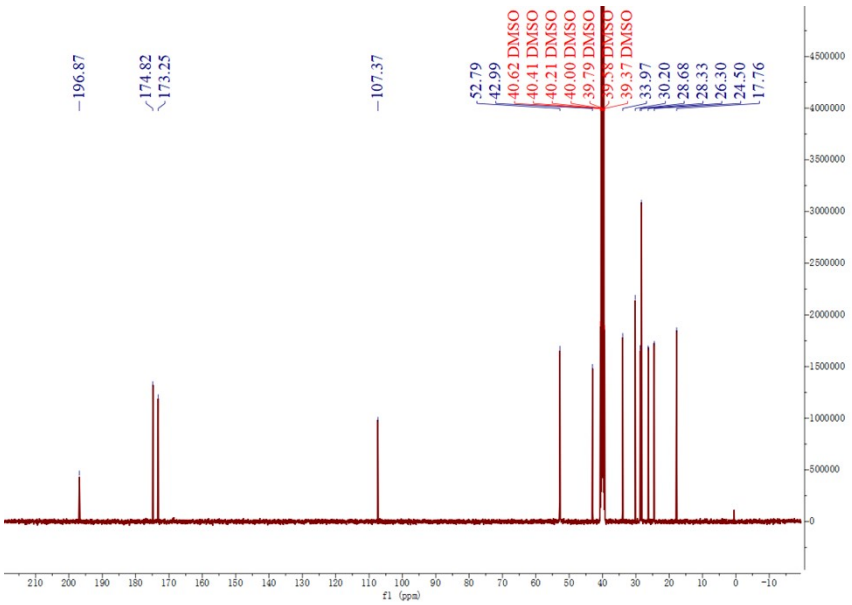

Fig. S40 ^{13}C NMR spectrum of **Dde-COOH-4** in DMSO-d_6.

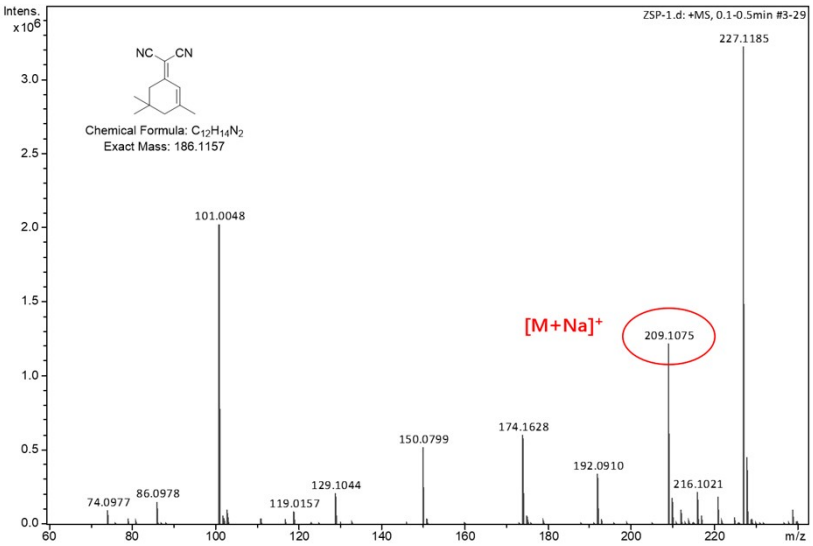

Fig. S41 HRMS spectrum of **DCI**.

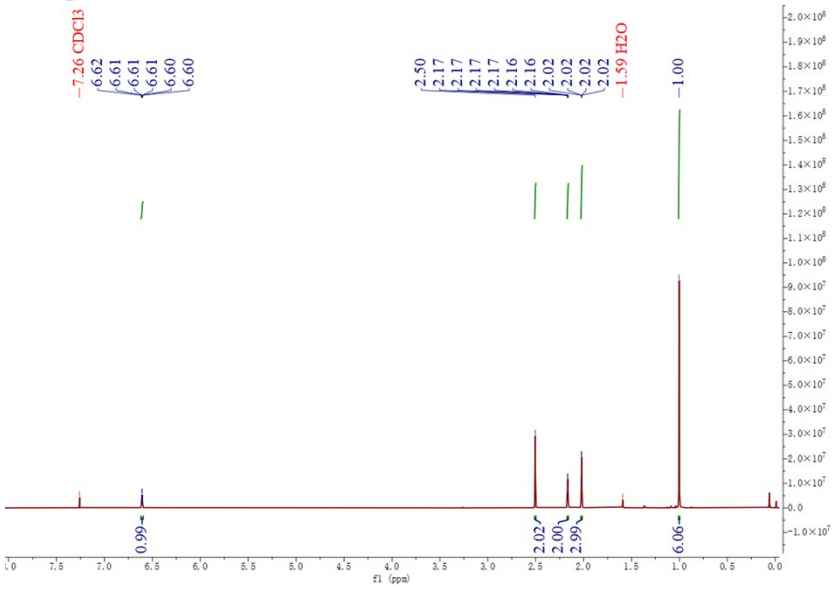

Fig. S42 ^{1}H NMR spectrum of **DCI** in $CDCl_3$.

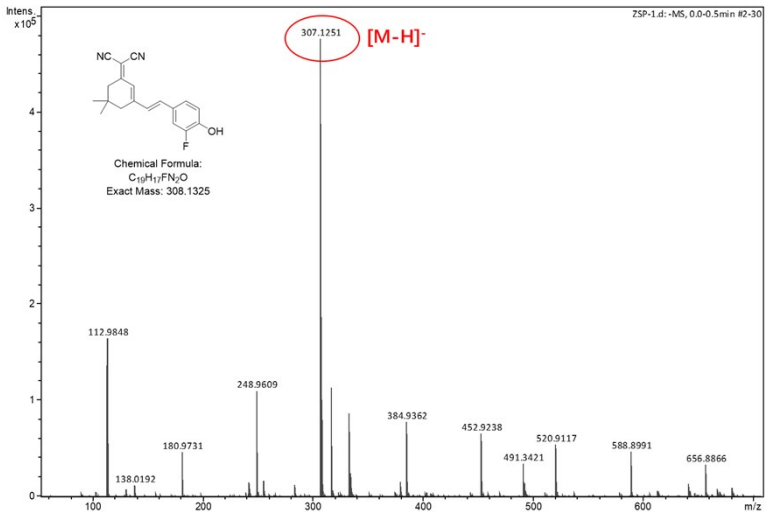

Fig. S43 HRMS spectrum of **DCI-OH**.

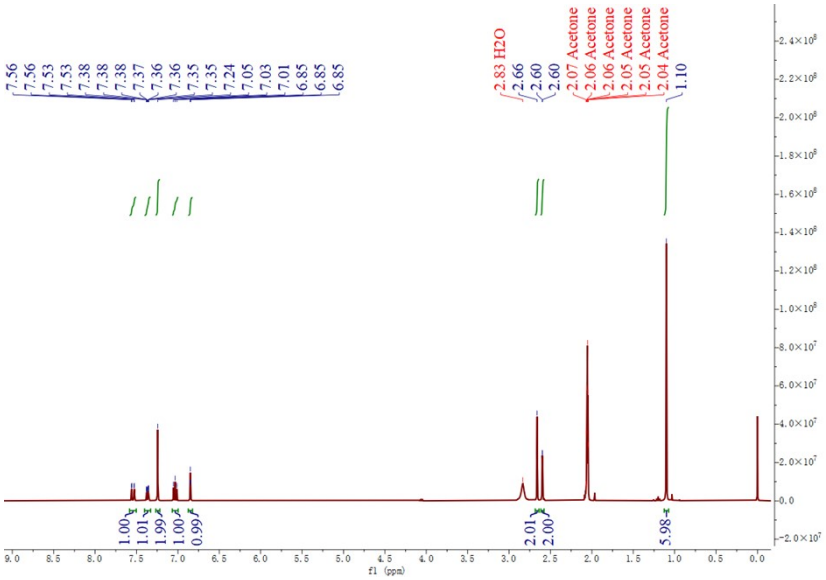

Fig. S44 ^{1}H NMR spectrum of **DCI-OH** in acetone-d_6.

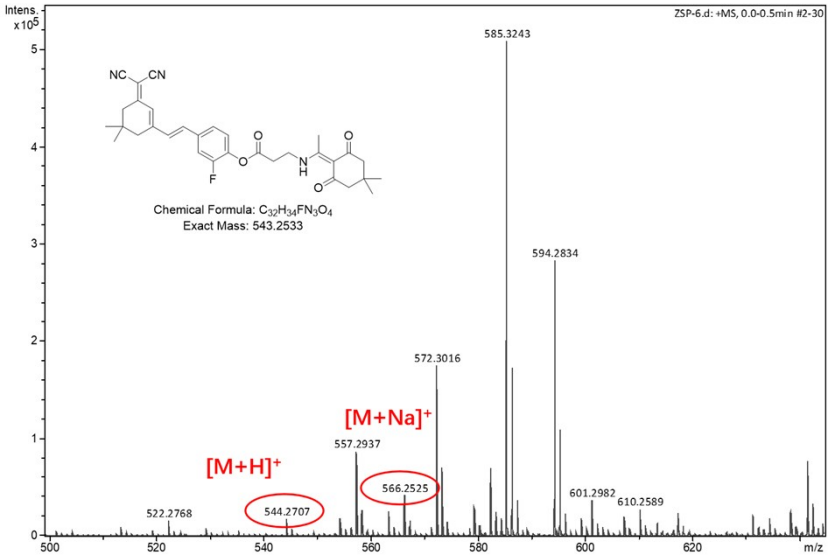

Fig. S45 HRMS spectrum of **DCI-HA-1**.

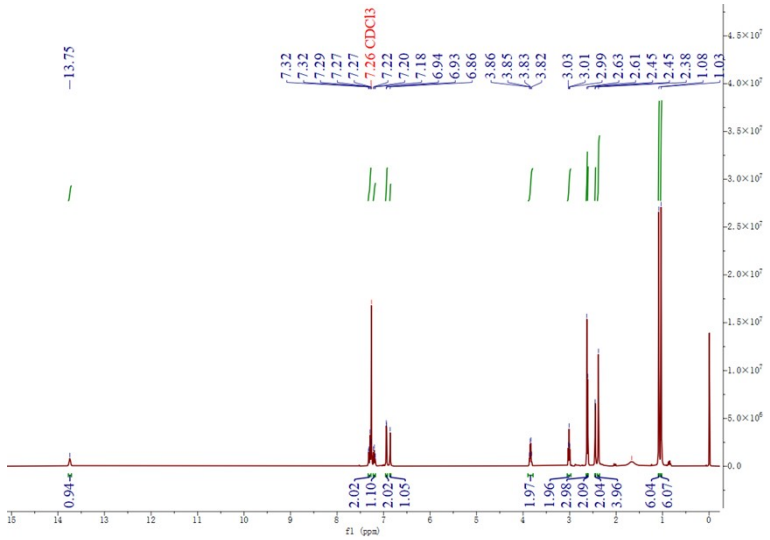

Fig. S46 ^{1}H NMR spectrum of **DCI-HA-1** in $CDCl_3$.

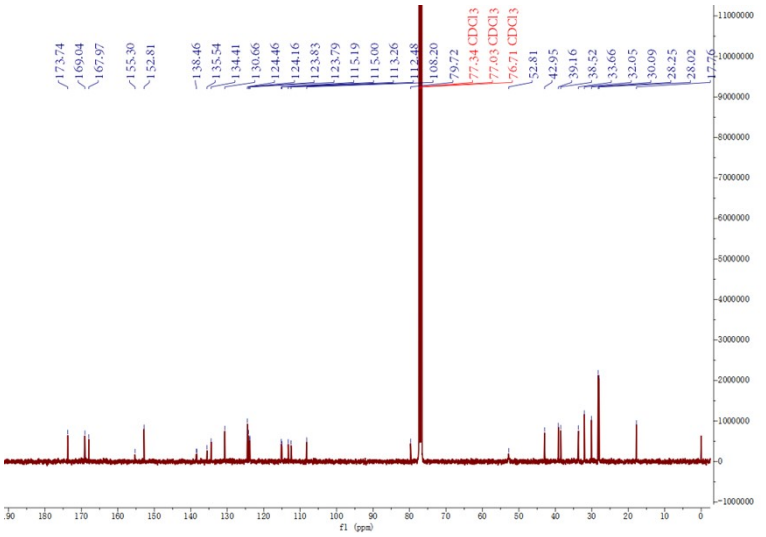

Fig. S47 ^{13}C NMR spectrum of **DCI-HA-1** in $CDCl_3$.

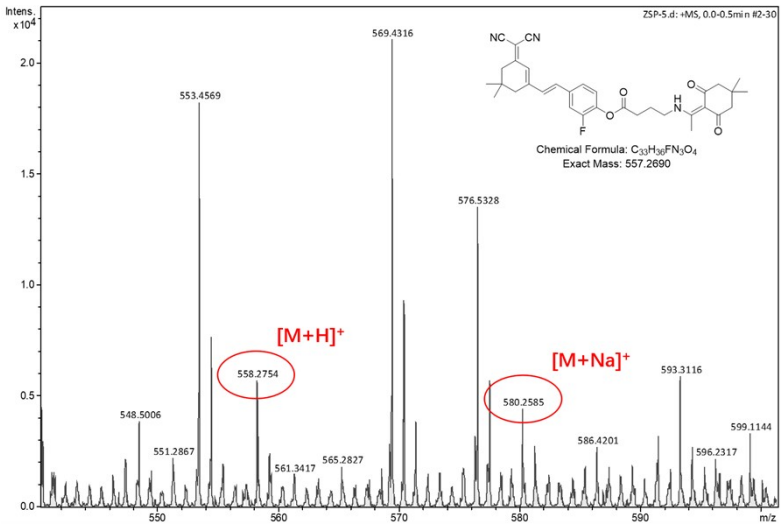

Fig. S48 HRMS spectrum of **DCI-HA-2**.

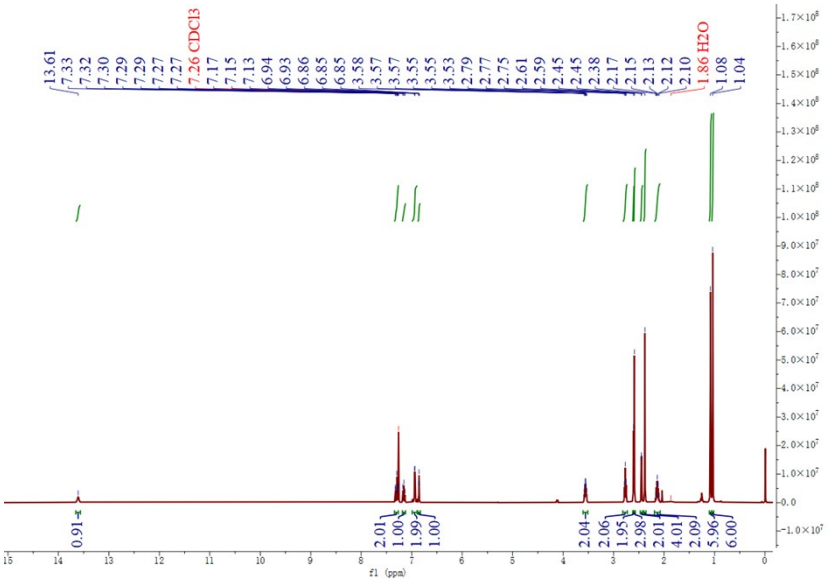

Fig. S49 ^{1}H NMR spectrum of **DCI-HA-2** in $CDCl_3$.

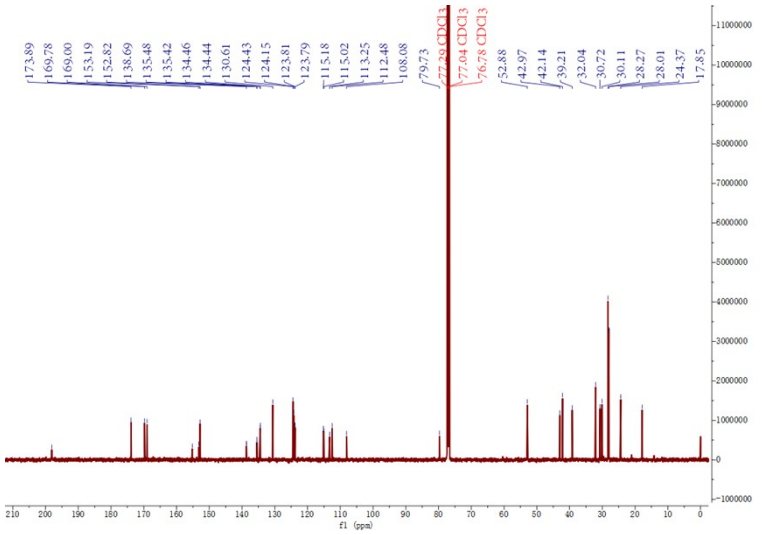

Fig. S50 ^{13}C NMR spectrum of **DCI-HA-2** in $CDCl_3$.

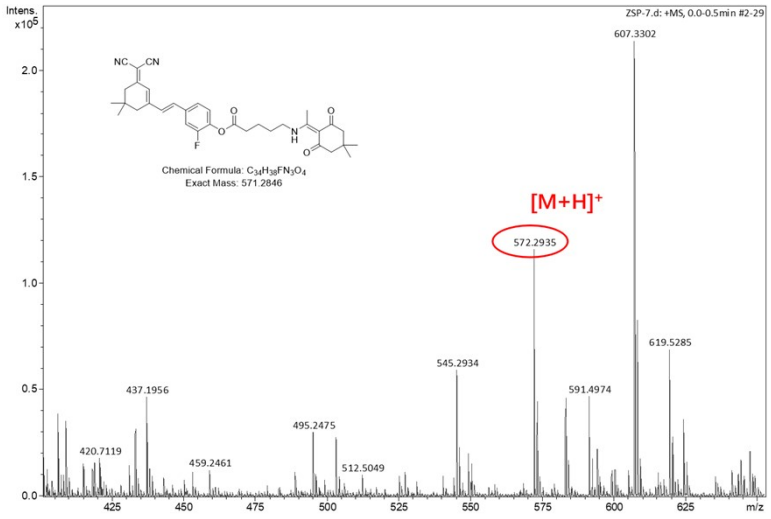

Fig. S51 HRMS spectrum of **DCI-HA-3**.

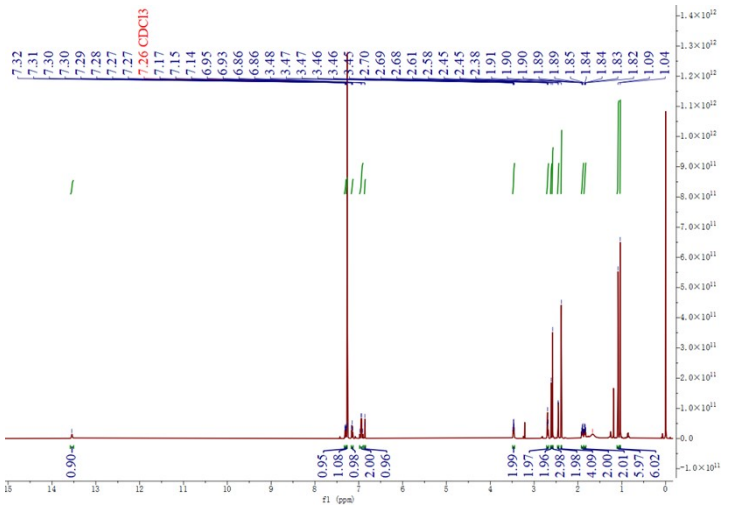

Fig. S52 ^{1}H NMR spectrum of **DCI-HA-3** in $CDCl_3$.

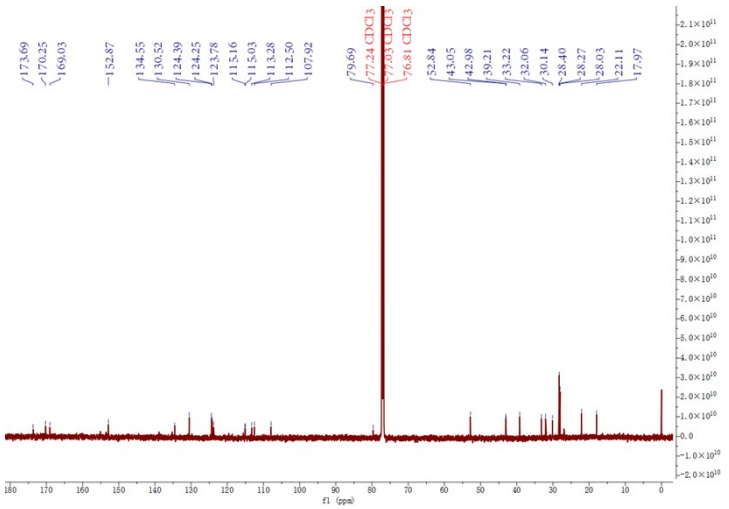

Fig. S53 ^{13}C NMR spectrum of **DCI-HA-3** in $CDCl_3$.

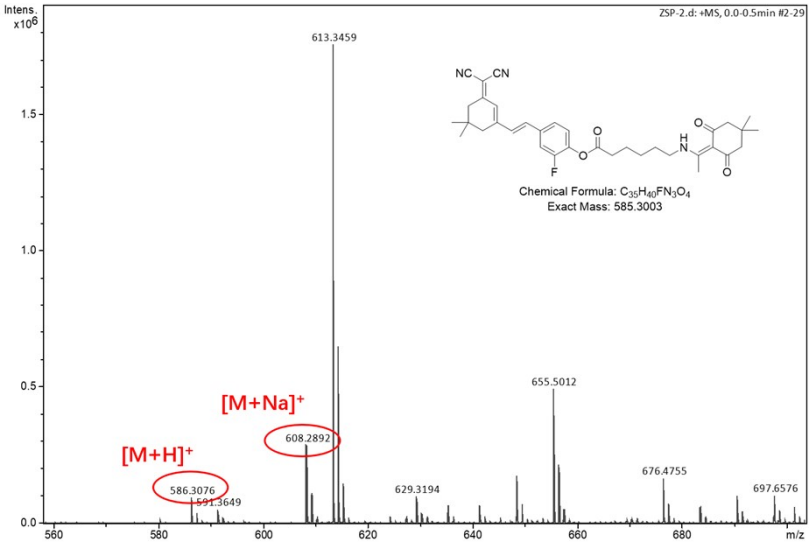

Fig. S54 HRMS spectrum of **DCI-HA-4**.

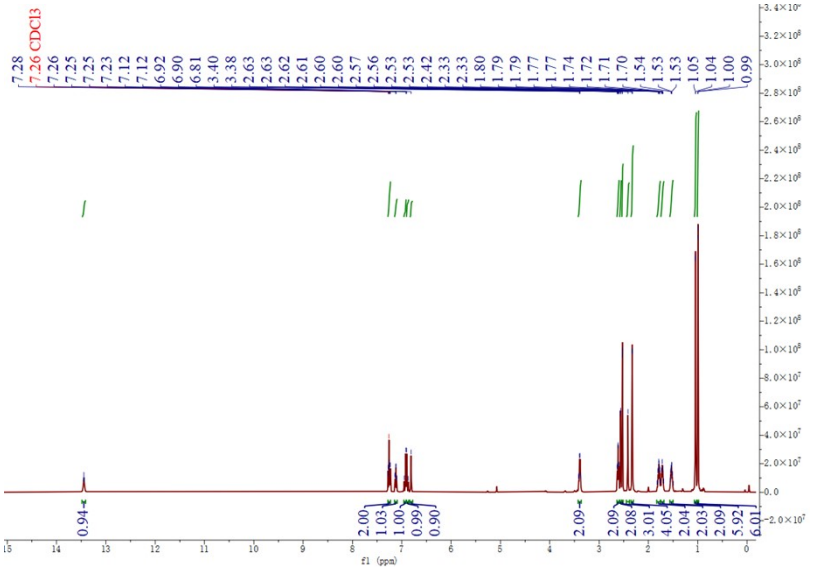

Fig. S55 ^{1}H NMR spectrum of **DCI-HA-4** in $CDCl_3$.

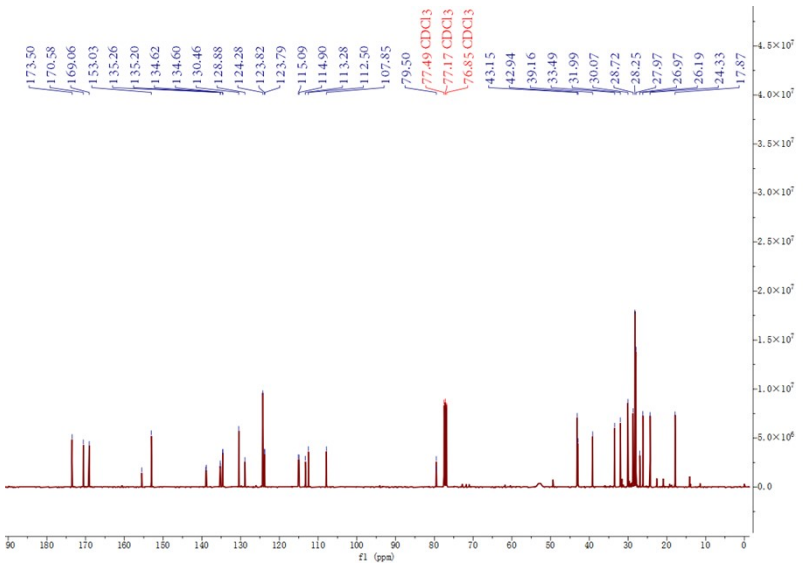

Fig. S56 ^{13}C NMR spectrum of **DCI-HA-4** in $CDCl_3$.

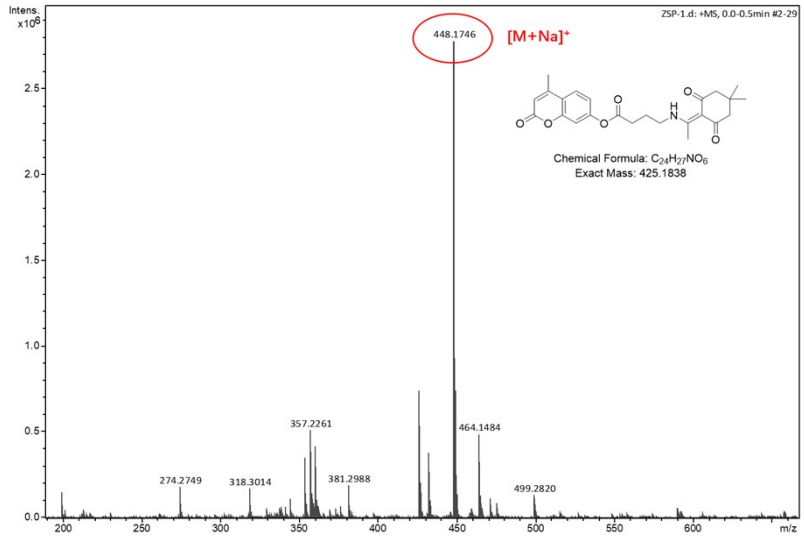

Fig. S57 HRMS spectrum of **Cou-HA**.

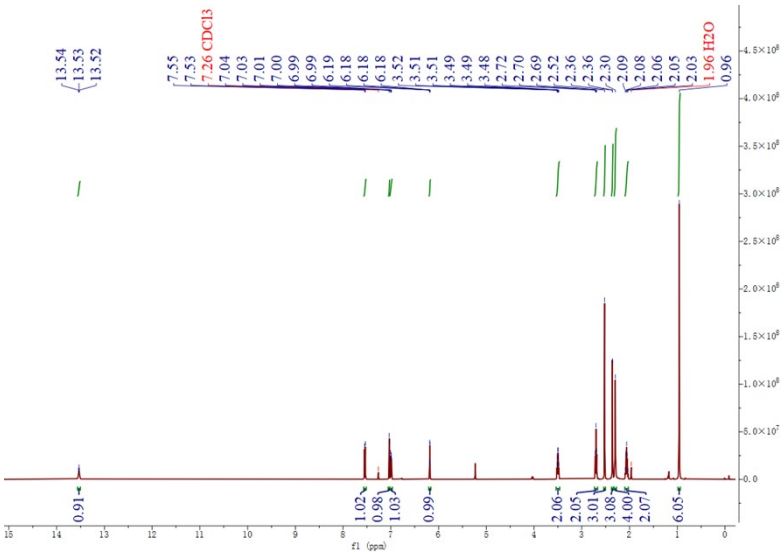

Fig. S58 ^{1}H NMR spectrum of **Cou-HA** in $CDCl_3$.

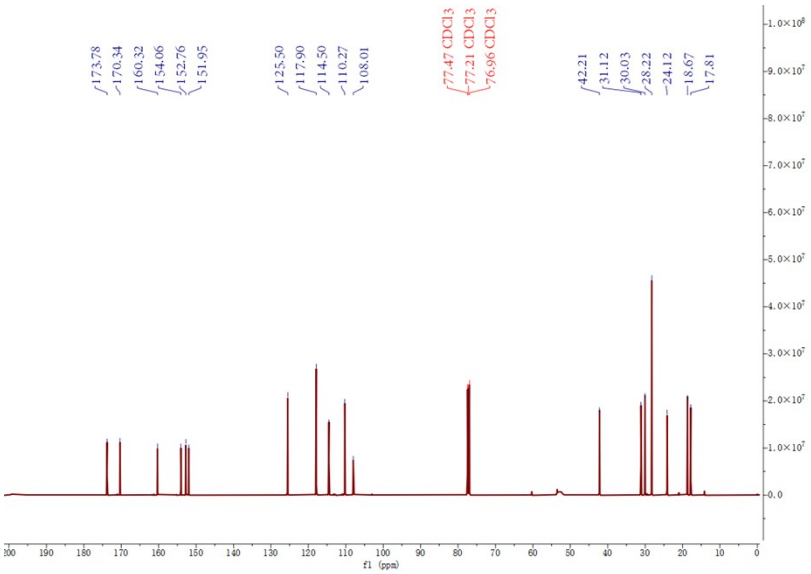

Fig. S59 ^{13}C NMR spectrum of **Cou-HA** in $CDCl_3$.

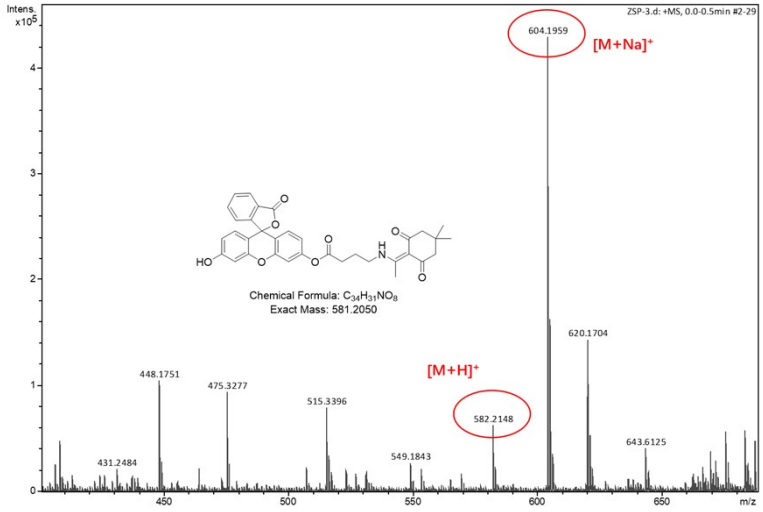

Fig. S60 HRMS spectrum of **Flou-HA**.

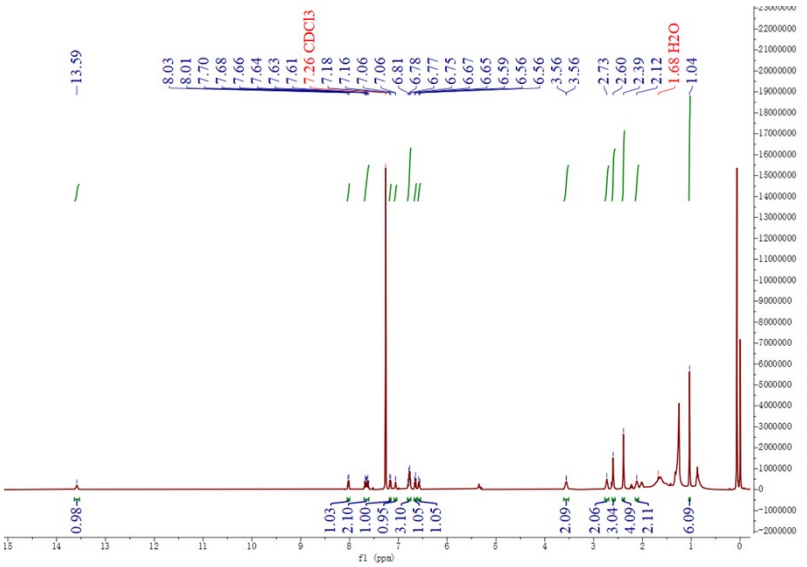

Fig. S61 ^{1}H NMR spectrum of **Flou-HA** in $CDCl_3$.

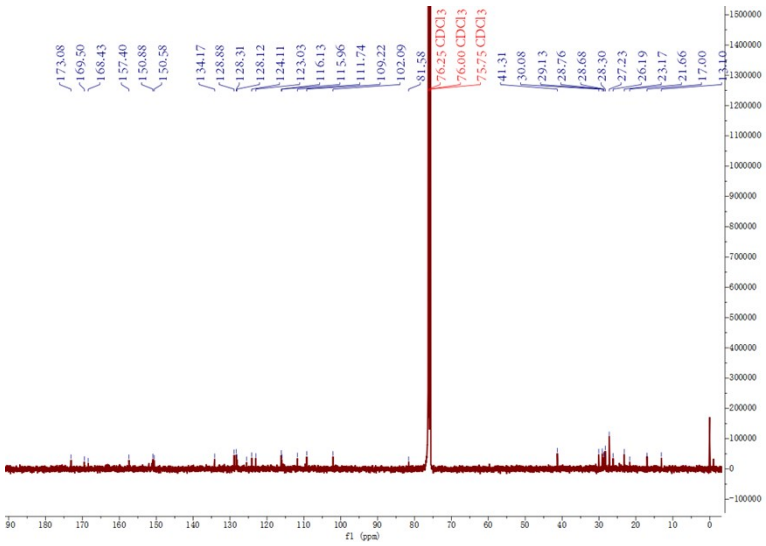

Fig. S62 ^{13}C NMR spectrum of **Flou-HA** in $CDCl_3$.

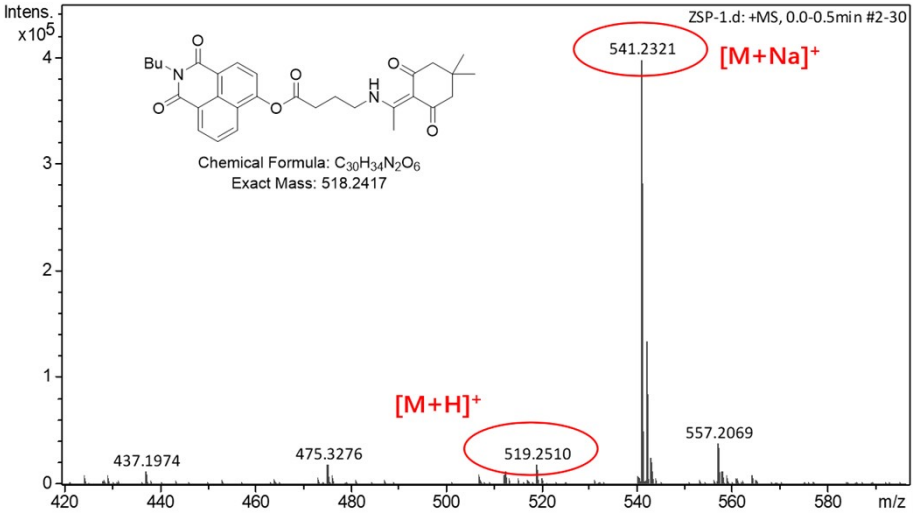

Fig. S63 HRMS spectrum of **Naph-HA**.

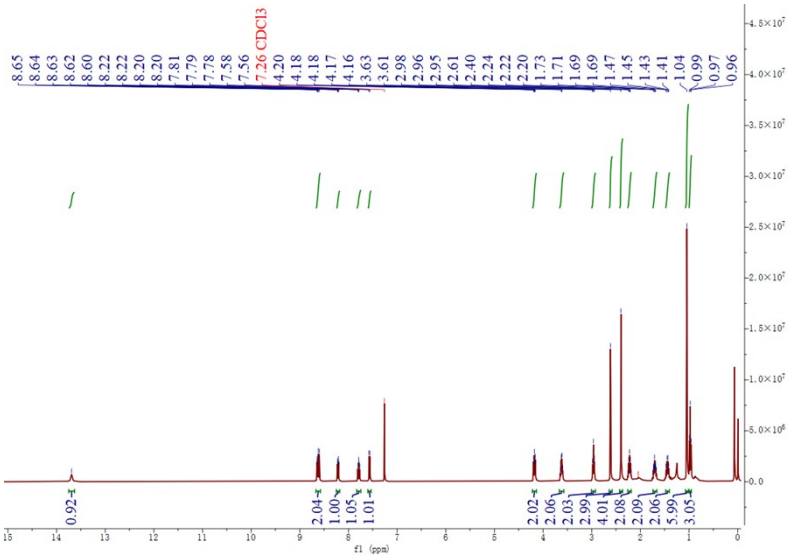

Fig. S64 ^{1}H NMR spectrum of **Naph-HA** in $CDCl_3$.

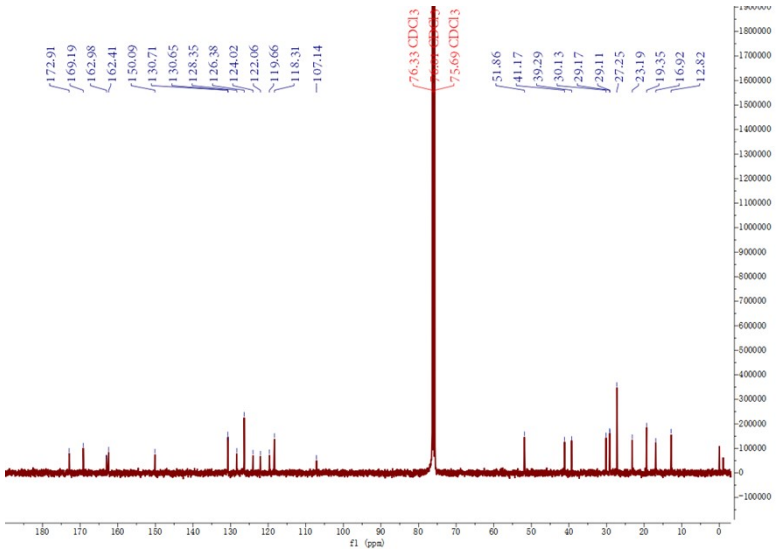

Fig. S65 ^{13}C NMR spectrum of **Naph-HA** in $CDCl_3$.

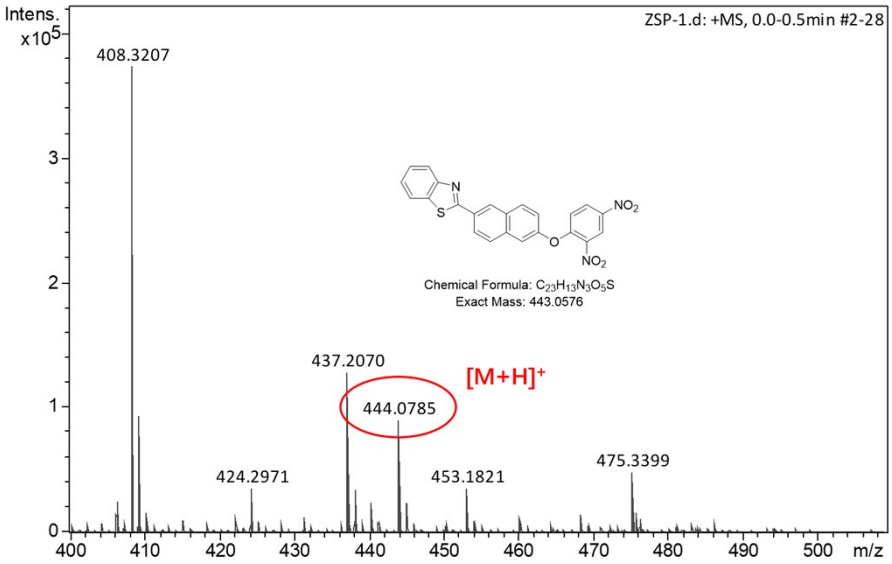

Fig. S66 HRMS spectrum of **N-H_2S**.

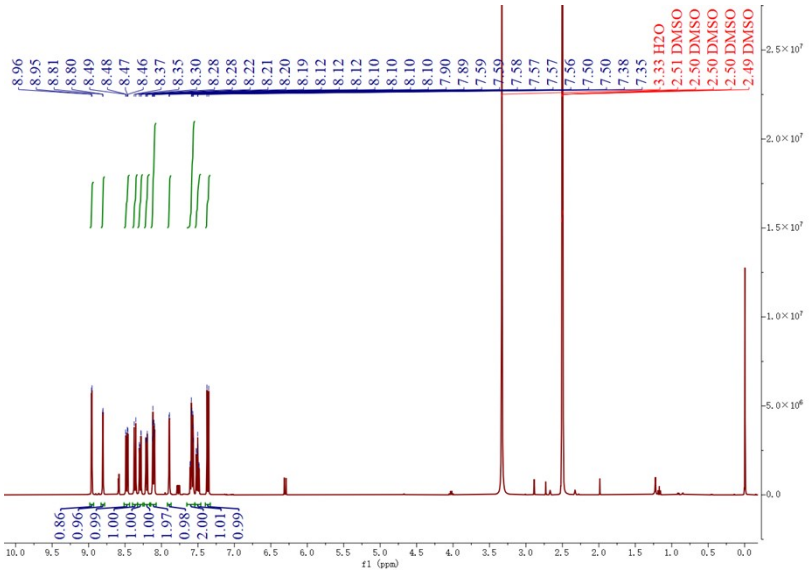

Fig. S67 ^{1}H NMR spectrum of **N-H_2S** in DMSO-d_6.

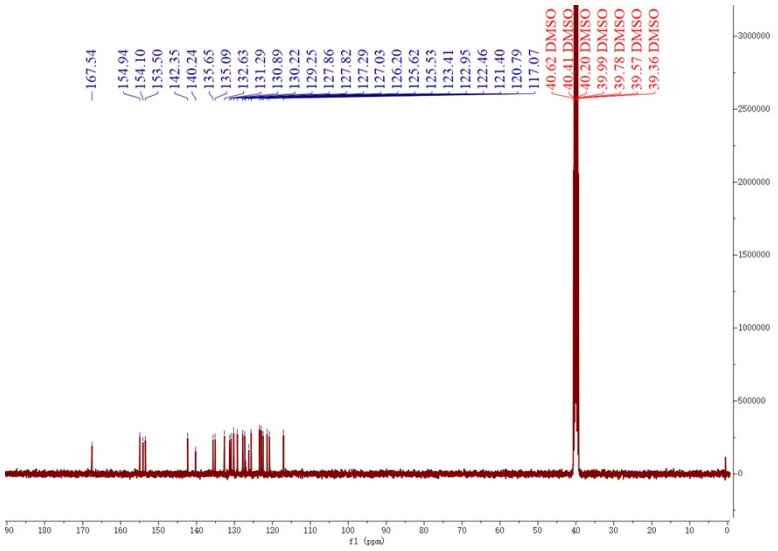

Fig. S68 ^{13}C NMR spectrum of **N-H_2S** in DMSO-d_6.